Geometry of Adinkra Embeddings

A Senior Project submitted to
The Division of Science, Mathematics, and Computing
of
Bard College

by
Andy Huynh

Annandale-on-Hudson, New York
December, 2014

Abstract

Adinkras are mathematical objects used to study supersymmetric objects, the two elementary particles called bosons and fermions in quantum mechanics. We can embed graphs on surfaces and study the induced geometry on them. Adinkras in particular can be embedded on Riemann surfaces with well understood structure. We build up the machinery required to embed adinkras into Riemann surfaces, then we use these tools to understand the geometry of specific adinkras after embedding into Riemann surfaces.

Contents

List of Figures

Dedication

To the many people who have impacted my life to make this possible,

- Patrick Honner,

- Kazue Kurahara,

- Toshiaki Jitsukawa,

- Jonathan Trombley.

Acknowledgments

This project wouldn't have existed without Greg Landweber's advising. There was much I learned from him, and much that he did to make the most out of my senior project.

With Greg's departure, this project wouldn't have been finished if Jim Belk didn't take over as advisor. There were many mathematical topics that I learned from him, and this project would have never been like this without his support.

Finally, the faculty and students of Bard College whom I've met during my time here, as their support and inspiration made my college experience worth remembering and instilled life into me again.

Introduction

Adinkras are graphs that contain information about off-shell supersymmetry. Adinkras have much structure to them, and have connections to both Clifford algebras and coding theory [4] [5]. There are many ways of studying adinkras. One such way is through their graph structure, a series of points and the links between them. But adinkras can also be considered as a combinatorial object and can be studied that way [21]. In addition to being graphs, adinkras are N-regular, N-edge-colored bipartite, with signed edges and heights assigned to vertices. Finally, we can consider error-correcting codes, and realize that there exists a link between them and adinkras [5] [11].

The authors of [5] observed that there are natural ways of embedding adinkras onto surfaces. The edge-coloring of an adinkra gives a cyclic ordering of the edges at each vertex of the graph based on their color. This ordering is called a *rainbow*. The only additional information needed to embed graphs into topological surfaces is a cyclic ordering of the edges at every vertex [8] [17], so the rainbow provides this ordering. In addition, adinkras can be realized as another type of graph called dessins d'enfants [5]. Grothendieck showed that any graph embedding has an associated complex structure, giving rise to a Riemann

surface [7] [12] [10]. As a result, any adinkra has an associated Riemann surface. This leads to the question of which geometry the Riemann surfaces have after embedding the adinkras. Two surfaces can be homeomorphic but geometrically distinct, as can be seen in the example of a torus. All tori are homeomorphic, but there exists a huge number of different tori geometrically.

An approach through geometry is one way to view Riemann surfaces, but another approach that will not be discussed is through algebraic curves. We can describe a torus using an algebraic curve, and we would be able find equations to the adinkra after embedding it on a torus.

We are interested in studying the geometry of adinkras. In particular, when we have a Riemann surface of genus 1 or greater, it has a Euclidean or hyperbolic structure. This makes it possible to ask questions such as what are the lengths of curves on these surfaces or what the angles are between curves on these surfaces. These questions can be applied to our adinkras after embedding.

The results in this project can be found mostly in chapter 5. In section 5.1, the key idea is that we use the symmetry of codes and their connections to adinkras to find that after embedding, the edges of adinkras are geodesic segments of equal length, as well as the angles between all adjacent pairs of edges are equal. This argument using symmetry is a strong one, but it can only be applied to specific adinkras. However, we find that all adinkras can be found as a quotient of adinkras with the most amount of symmetry by doubly-even codes. From there, we can extend our argument to all adinkras.

In section 5.2, we find results for adinkras whose number of edge colors are between 2 and 4. In the case of the $N = 2$ adinkra, we actually are able to find a function that maps the adinkra onto the surface, which in this case is the Riemann sphere, and figure out its geometry that way. For the $N = 3$ adinkra, we also have an embedding into the Riemann sphere and study its geometry as well. For the $N = 4$ adinkras, we have two adinkras,

both of which embed onto a torus. Since the complex structure of a torus is Euclidean, we are able to study its geometry quite easily.

In section 5.3, we study an $N = 5$ adinkra. We find that this adinkra embeds onto a 3-holed torus, and the complex structure of such a torus is hyperbolic. We first begin by figuring out the geometry of the adinkra after embedding. Then we try to find out the geometry of the 3-holed torus itself. The universal cover of a 3-holed torus is the hyperbolic plane. As a result, we use Fuchsian groups to find Dirichlet regions. The Dirichlet regions end up helping us find fundamental regions for our 3-holed torus. We study two fundamental regions, one that is polygonal with 16-sides, and another that is dodecagonal. The fundamental region with the least number of sides for a 3-holed torus is indeed a dodecagon. The geometry of these fundamental region that we find are the edge lengths of these regions, as well as the interior angles.

In section 5.4, we show that our symmetry argument used to understand adinkra embeddings is strong enough that it can be used to find out the geometry of adinkras after embedding even if we did not figure out what the actual embedding is. Then we end by discussing other ways of embedding adinkras onto surfaces and how that affects our arguments.

1
Adinkras

The main purpose of this chapter will be to explain adinkras and other important properties that will be used. Before stating what an adinkra is, we will mention that adinkras are a mathematical structure inspired by finding a way to mathematically represent a phenomenon in physics. The rest of the paper will focus on adinkras from a mathematical point of view, so there will be no more mention of this background from physics.

1.1   Adinkra Definition

We begin by discussing graphs and special kinds of graphs. This is necessary as adinkras are actually graphs that satisfies these properties, along with additional properties that define them. We can view graphs as a series of points and connections that link these points.

Definition 1.1.1. A *graph* G is a pair of sets V, E such that V is not empty and E is a set of two element subsets of V. The set V is known as the *vertices* of G, and the set E is known as the *edges* of G. $\triangle$

Definition 1.1.2. A graph is *bipartite* if there exists a partition of the set of vertices into two sets A, B such that every edge connects a vertex in A to a vertex in B. △

We can now give examples of specific types of graphs.

Example 1.1.3. A graph that connects every possible pair of vertices is called *complete*, denoted by K_p where p is the number of vertices. Complete graphs resemble polygons with all diagonals drawn. A *complete bipartite graph* is denoted by $K_{m,n}$ where m, n are the number of vertices in the two partition sets of the vertices. ◇

With these definitions of special types of graphs, we can now begin to build towards adinkras in particular. Before that, we want to have notation that allows us to specify the edges and vertices of a graph. Let G be a graph. Then we denote the edges of the graph by $E(G)$ and the vertices by $V(G)$. Information here can also be found in [21].

Definition 1.1.4. An *adinkra* A is a graph together with a *ranking function h* and a set $\mathcal{E} \subset E(A)$ of *dashed edges* that satisfies the following properties.

1. A is a finite graph.

2. A is a connected graph.

3. A is a bipartite graph.

4. A is N-regular, meaning that every vertex is connected to exactly N edges.

5. There are N distinct colors that the elements of $E(A)$ are colored by, such that every vertex is connected to exactly one edge of each color.

6. For any two distinct colors, the edges colored by those two colors form disjoint 4-cycles.

7. The ranking is a function $h\colon V(A) \to \mathbb{N}$ such that any two connected vertices differ by exactly one rank. In adinkra diagrams, rankings are represented by height placement.

8. For every 4-cycle, an odd number of edges are in $\mathcal{E}$. $\triangle$

We will not explicitly be using the ranking or the dashing in this project, though we will be using the resulting classification of adinkras 1.2.10.

Definition 1.1.5. An *adinkra topology* is the graph structure of an adinkra, i.e., we remove the edge coloring, vertex ranking, and edge dashings of an adinkra. $\triangle$

Definition 1.1.6. An *adinkra chromotopology* is the graph structure of an adinkra with edge colorings, i.e., we remove the vertex ranking, and edge dashings of an adinkra. $\triangle$

An adinkra topology can simply be called a topology for short. Similarly, an adinkra chromotopology can be simply be called a chromotopology.

We want an easy way to categorize adinkras. For each adinkra topology, we can attach two numbers, as follows.

Definition 1.1.7. The *degree N* of an adinkra topology is the number of edges that each edge has. $\triangle$

Proposition 1.1.8. *If A is an adinkra of degree N, then A has 2^n vertices for some integer $n \leq N$.*

Proof. This is comes from the classification of adinkras using codes from proposition 1.2.10. $\square$

An adinkra with 2^n vertices is said to have *dimension n*.

Example 1.1.9. The graph of a cube is called the cube adinkra as shown in figure 1.1.1. $\lozenge$
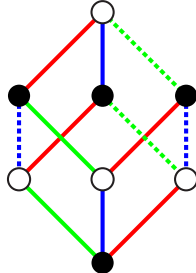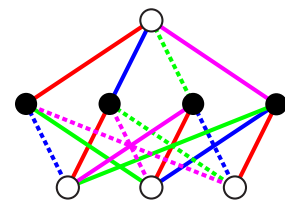
Figure 1.1.1: The cube adinkra.

Figure 1.1.2: This is the adinkra with $K_{4,4}$ topology.

Example 1.1.10. The graph $K_{4,4}$ is an adinkra as shown in figure 1.1.2. ◇

1.2 Codes and Adinkras

Another perspective of understanding adinkras is through the world of coding theory. There are many types of codes, but the ones that are most useful are linear codes, having nice properties that make them use to use in practical applications. Three very common linear codes may be n-tuples of $\mathbb{Z}_2, \mathbb{Z}_3$ and $\mathbb{Z}_4$. However, the one relevant to adinkras are binary codes, the n-tuples of $\mathbb{Z}_2$. The information on codes come from [11].

Definition 1.2.1. Let $\mathbb{Z}_2^n$ be a vector space over $\mathbb{Z}_2$. Then an $[n, k]$ *code* $\mathcal{C}$ is a subspace of $\mathbb{Z}_2^n$ with dimension k. The elements of $\mathcal{C}$ are called *codewords*. A *subcode* of $\mathcal{C}$ is a subset of $\mathcal{C}$ that is also a code. △

Definition 1.2.2. The *weight* of a codeword is its digit sum. △

Definition 1.2.3. A codeword is *even* if its weight is even. △

Definition 1.2.4. A codeword is *doubly-even* if its weight is a multiple of four. A code is doubly-even if all codewords are doubly-even. △

Example 1.2.5. The set $\{000, 001, 010, 011, 100, 101, 110, 111\}$ form a code. ◇

Example 1.2.6. Let $e_i \in \mathbb{Z}_2^N$ be the codeword that is 1 in the i'th coordinate and 0 for all other coordinates. Then the span of $\{e_i\}$ is a code. ◇

Example 1.2.7. The span of $\{1000011, 0100101, 0010110, 0001111\}$ form a code. This is an example of something called the $[7, 4]$ Hamming code. $\Diamond$

Now we need to identify a notion of when two codes are essentially the same. All that we want are codes that are equivalent under permutation.

Definition 1.2.8. Two codes $\mathcal{C}_1, \mathcal{C}_2$ are *permutation-equivalent* if there exists a permutation matrix P such that for every $c_1 \in \mathcal{C}_1$, there exists a $c_2 \in \mathcal{C}_2$ such that $Pc_1 = c_2$. $\triangle$

Now we can specify the relation between adinkras and codes. This information can be found in [5] and [6].

Definition 1.2.9. We will let I_N be the N-cube graph, which is defined as follows:

1. Vertices of I_N correspond to codewords of $\mathbb{Z}_2^N$.

2. Edges of I_N link 2 codewords that differ in exactly one coordinate. $\triangle$

Let $\mathcal{C}$ be a subcode of $\mathbb{Z}_2^N$. This subcode acts on I_N by automorphisms of the graph. It is easy to see that the action of the subcode does not have any fixed vertices or edges, so we can take the quotient of I_N by $\mathcal{C}$. When we take the quotient by certain subcodes, it turns out that the resulting code can still be found to correspond to an adinkra.

Proposition 1.2.10. *An n-dimensional, N-degree adinkra is isomorphic to the quotient of I_N by a doubly-even subcode of $\mathbb{Z}_2^N$.*

As adinkras grow in dimension, the number of vertices increase exponentially, and it becomes more difficult to even generate. So, using coding theory, we can overcome this, as we can instead look at more familiar structures, which are basically quotients of n-tuples of $\mathbb{Z}_2$. This way, we can name every single vertex, identify all of the edges, and even identify edge colors without needing to make sure that all of the properties of the adinkra are satisfied.
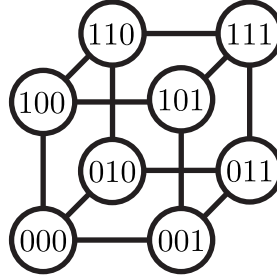
Figure 1.2.1: A graph with the cube adinkra topology with vertices labeled as their corresponding codes.

Example 1.2.11. There are two adinkras that can be formed from I_4. The two codes that form them are the trivial doubly-even code $\{0000\}$ and the only non-trivial doubly-even subcode $\{0000, 1111\}$ of length 4. Thus, the two adinkras are $I_4/\{0000\}$ and $I_4/\{0000, 1111\}$. $\diamond$

Example 1.2.12. There are two 5-dimensional adinkras. One has 16 vertices and 40 edges. This is the quotient of I_5 and the code $\{00000, 11110\}$. The other has 32 vertices. This is $I_5/\{00000\}$. $\diamond$

Now that we have developed a notion of what adinkras are, we will now talk about specific examples of them to get a better understanding of what will we try to study. As we will focus on adinkra chromotopologies, we will not talk about edge dashings and rankings.

First, we have the most trivial adinkra, one with 2 vertices and one edge. There is one edge color. This is isomorphic to I_1. The next are square adinkras. They have 4 vertices and 4 edges. There are two edge colors. This is isomorphic to I_2. The cube adinkra has 8 vertices and 24 edges. There are 3 edge colors and is isomorphic to I_3.

There are now two possible paths to go from here. We can increase the number of vertices, but another possible path is to increase the number of edges. There are 8 vertices

n	N	Vertices	Edges	Code Isomorphism Type
1	1	2	1	I_1
2	2	4	4	I_2
3	3	8	12	I_3
3	4	8	16	$I_4/\{0000, 1111\}$
4	4	16	32	I_4
4	5	16	40	$I_5/\{00000, 11110\}$
5	5	32	80	I_5
4	6	16	48	$I_6/\{000000, 111100, 001111, 110011\}$
5	6	32	96	$I_6/\{000000, 111100\}$
6	6	64	192	I_6

Table 1.2.1: A table of low dimensional adinkras, their degrees, number of vertices, number of edges, and isomorphism type.

and 4 edges per vertex. This adinkra is isomorphic to the $I_4/\{0000, 1111\}$. Note that before this point, there did not exist any nontrivial doubly even codes.

Now that we have exhausted all of our vertices, the only path left to take is to increase the number of vertices. So now we have 16 vertices, but there are still 4 edges per vertex. This adinkra is isomorphic to I_4.

We will now increase the number of edges per vertex, leading to our next example of an adinkra with 16 vertices and 5 edges per vertex, resulting in having a total of 40 edges. This is the same as $I_5/\{00000, 11110\}$.

For our final examples, we will talk about adinkras of degree 6. The code I_6 has only 3 doubly-even subcodes. They are

$$\{000000\}, \{000000, 111100\}, \{000000, 111100, 110011, 001111\},$$

up to permutation-equivalence. Thus, our three adinkras of degree 6 are the quotients of I_6 by each of these three doubly-even subcodes.

These are the small adinkra chromotopologies up to isomorphisms. For a complete classification of adinkra chromotopologies, refer to [6].

2

Topology and Complex Analysis

From here, we want to discuss how adinkras relate to topological surfaces. In order to do that, we need to talk about the classification of compact surfaces. But to do that, we need to know what each of these things mean. We will assume the reader knows basic topology and complex analysis, along with basic homotopy and fundamental groups. Resources to learn these materials in an introductory manner include [18] and [1].

2.1   Topological Surfaces and Manifolds

In order for us to relate adinkras to surfaces, we need to talk about what surfaces are. We will build a foundation for surfaces that works as well as have a practical purpose in order to extend to other examples quite easily. The material here is adapted from [16].

Definition 2.1.1. Let X be a topological space. A *coordinate chart* or just chart is a homeomorphism $\phi\colon U \to V$, where $U \subset X$ is an open set in X and $V \subset \mathbb{R}^2$ is an open set in $\mathbb{R}^2$. $\triangle$

Example 2.1.2. Let X be the unit sphere. Let $U \subset X$ be the upper half of the sphere without the boundary. Let $\phi_U \colon U \to \mathbb{R}^2$ by $\phi_U(x, y, z) = (x, y)$. In other words, the function ϕ projects the upper half of the sphere to the plane. Then ϕ_U is a chart. $\quad \diamond$

Example 2.1.3. Let X be a topological space. Let $\phi \colon U \to V$ be a chart on X. Let $\psi \colon V \to W$ be a homeomorphism between two open sets in $\mathbb{R}^2$. Then $\psi \circ \phi \colon U \to W$ is a chart on X. This example can be known as a *change of coordinates*. $\quad \diamond$

Note that the domain of a single chart may simply be a subset of a topological space X. We may need to have a collection of charts in order for our charts to be useful for all of X. This brings up the notion of an atlas.

Definition 2.1.4. An *altas* $\mathcal{A}$ on X is a collection $\{\phi_\alpha \colon U_\alpha \to V_\alpha \mid U_\alpha \subset X, V_\alpha \subset \mathbb{R}^2\}$ of charts whose domains cover X, i.e, $X = \bigcup_\alpha U_\alpha$. $\quad \triangle$

Now we are ready to define a surface. Note that an atlas gives some sort of a structure to a topological space, and this is how surfaces will be defined.

Definition 2.1.5. A topological space X that is Hausdorff, second countable, and has at least one atlas is a *surface*. More generally, a topological space X that is Hausdorff, second countable, and has at least one atlas of charts mapping open subsets of X to $\mathbb{R}^n$ is a *manifold*. $\quad \triangle$

Example 2.1.6. Let $X = \mathbb{R}^2$ be a topological space with the standard topology. Let the atlas consist of a chart $\phi \colon \mathbb{R}^2 \to \mathbb{R}^2$ by the identity map. Then X is a surface trivially. $\quad \diamond$

Example 2.1.7. Let $S^2 = \{(x, y, z) \in \mathbb{R}^3 \mid x^2 + y^2 + z^2 = 1 \in \mathbb{R}\}$ be the unit sphere. Let $\phi_1 \colon S^2 \smallsetminus \{(0, 0, 1)\} \to \mathbb{R}^2$ be a chart on S^2 defined by

$$\phi_1(x, y, z) = \left(\frac{x}{1 - z}, \frac{y}{1 - z} \right).$$

The inverse function is

$$\phi_1^{-1}(x, y) = \left(\frac{2x}{1 + x^2 + y^2}, \frac{2y}{1 + x^2 + y^2}, \frac{x^2 + y^2 - 1}{1 + x^2 + y^2} \right).$$

Let $\phi_2 \colon S^2 \smallsetminus \{(0, 0, -1)\} \to \mathbb{R}^2$ be another chart on S^2 by

$$\phi_2(x, y, z) = \left(\frac{x}{1 + z}, -\frac{y}{1 + z} \right).$$

The inverse function is

$$\phi_2^{-1}(x, y) = \left(\frac{2x}{1 + x^2 + y^2}, -\frac{2y}{1 + x^2 + y^2}, \frac{1 - x^2 - y^2}{1 + x^2 + y^2} \right).$$

These two charts form an atlas, and thus the sphere is a surface. $\diamond$

Example 2.1.8. Let X be a surface with atlas $\mathcal{A} = \{\phi_\alpha \colon U_\alpha \to V_\alpha\}$. Any open subset Y of X is also a surface by the atlas $\mathcal{A}_Y = \{\phi_\alpha|_{Y \cap U_\alpha} \colon Y \cap U_\alpha \to \phi_\alpha(Y \cap U_\alpha)\}$. $\diamond$

The definition of surfaces can cover a broad range of objects. Some surfaces may not be desirable for they may have strange properties. We will talk about surfaces that are well behaved.

Definition 2.1.9. A surface is *closed* if it is compact and has no boundary. $\triangle$

Example 2.1.10. The plane is not a closed surface because it is not compact. A finite cylinder is compact, but it has a boundary, so it is not a closed surface. A sphere is compact and has no boundary, so it is a closed surface. Note that a closed surface is different from being closed in a topological sense. $\diamond$

We will now try to generalize surfaces and manifolds by talking about manifolds where we can somehow differentiate it. We will redefine our previous definitions in such a way that we can define a manifold with some notion of differentiability.

Definition 2.1.11. A *n-dimensional real chart* is a homeomorphism $\phi \colon U \to V$ where $U \subset X$ is an open set in X and V is an open set in $\mathbb{R}^n$. $\triangle$

In general, it is very easy to get one chart and produce another chart in an almost trivial way. These two charts are seemingly the same and in effect, both charts should produce the same answers when we ask questions such as questions about local functions. In the case of topological manifolds, this is not an issue, but now with the requirement of differentiability, this can be. We will now address this with the following definition.

Definition 2.1.12. Two real charts ϕ_1, ϕ_2 are $\mathcal{C}^\infty$-*compatible* if the function $\phi_2 \circ \phi_1^{-1} \colon \phi_1(U_1 \cap U_2) \rightarrow \phi_2(U_1 \cap U_2)$ is a $\mathcal{C}^\infty$ diffeomorphism. (Recall that a $\mathcal{C}^\infty$ function is a function that is infinitely differentiable.) $\triangle$

Definition 2.1.13. A $\mathcal{C}^\infty$ *atlas* is a collection of real charts that are pairwise $\mathcal{C}^\infty$ compatible and whose domains cover X. $\triangle$

Here, we have a new definition that we could have defined for topological manifolds but was not necessary. This definition brings an equivalence class of when two atlases, for it is definitely possible to have two different atlases be effectively the same.

Definition 2.1.14. A $\mathcal{C}^\infty$ *structure* is an equivalence class of $\mathcal{C}^\infty$ atlases. $\triangle$

Definition 2.1.15. An $\mathcal{C}^\infty$ *surface* is a surface with a $\mathcal{C}^\infty$-structure. $\triangle$

2.2 Riemann Surfaces

Instead of differentiable manifolds, we can impose other conditions that a surface needs to satisfy. This section will focus on complex differentiability.

While we have focused so far on real manifolds, we can very easily switch to complex manifolds by noting that $\mathbb{R}^2$ and $\mathbb{C}$ are homeomorphic. But before we can continue, we need to talk about differentiation in the complex plane.

Definition 2.2.1. Let $U \subset \mathbb{C}$. A function $f \colon U \to \mathbb{C}$ is *holomorphic* if for each $x \in U$, there exists an open set containing x such that all points in the open set is complex differentiable. $\triangle$

Definition 2.2.2. A function $f \colon U \to \mathbb{C}$ is *anti-holomorphic* if $f(\overline{z})$ is holomorphic, where $\overline{z}$ denotes the complex conjugate of z. $\triangle$

From here, we simply provide the same definitions as before, but now can be applied to holomorphic functions.

Definition 2.2.3. A *complex chart* is a homeomorphism $\phi \colon U \to V$ where $U \subset X$ is an open set in X and V is an open set in $\mathbb{C}$. $\triangle$

From the definition of complex chart, we can find obtain the corresponding definitions for a complex atlas and complex structure. Once we have figured those out, we can define what a Riemann surface is.

Definition 2.2.4. Two complex charts ϕ_1, ϕ_2 are *complex compatible* if the function $\phi_2 \circ \phi_1^{-1} \colon \phi_1(U_1 \cap U_2) \to \phi_2(U_1 \cap U_2)$ is holomorphic, and $\phi_1 \circ \phi_2^{-1} \colon \phi_2(U_1 \cap U_2) \to \phi_1(U_1 \cap U_2)$ is also holomorphic. $\triangle$

Definition 2.2.5. A *complex atlas* is a collection of complex charts that are pairwise complex compatible and whose domains cover X. $\triangle$

Definition 2.2.6. A *complex structure* is an equivalence class of complex atlases. $\triangle$

Definition 2.2.7. A surface X together with a complex structure is a *Riemann surface*. $\triangle$

Example 2.2.8. The complex plane with the identity map as a chart forms a Riemann surface. $\Diamond$

Example 2.2.9. Open subsets of the complex plane are also Riemann surfaces. The atlas of these Riemann surfaces contain one chart, which is just the identity map. Important

examples include the upper half-plane $\mathbb{H} = \{z \in \mathbb{C} \mid \text{Im}(z) > 0\}$ and the unit disc

$\mathbb{D} = \{z \in \mathbb{C} \mid |z| < 1\}$. ◊

Example 2.2.10. Similar to real surfaces, the unit sphere with a two chart atlas forms a Riemann surface. The two charts are similar to the charts in example 2.1.7, but slightly modified to the complex plane. The two charts are

$$\phi_1(x, y, z) = \frac{x + iy}{1 - z}, \qquad \phi_2(x, y, z) = \frac{x - iy}{1 + z}.$$

A unit sphere with this atlas is known as the *Riemann sphere*. There are many ways to denote the Riemann sphere, including $\mathbb{C} \cup \{\infty\}, \widehat{\mathbb{C}}, \mathbb{P}^1(\mathbb{C})$, and $\mathbb{CP}^1$. We shall use $\widehat{\mathbb{C}}$. ◊

Example 2.2.11. We can create a torus as a Riemann surface. Let $\Lambda = \{\mathbb{Z} \oplus \mathbb{Z}i\}$ be a lattice in the complex plane. Then $X = \mathbb{C}/\Lambda$ is a complex torus. Every open unit square with sides parallel to the axes in $\mathbb{C}$ maps homeomorphically to an open subset of X, and the inverses of these form an atlas. ◊

We shall conclude this section by stating that just like surfaces, Riemann surfaces can also be extended to higher dimensions. The definitions are exactly as one would expect and increasing the number of dimensions does not bring anything that we need to be careful of. However, since we will not be using higher dimensional complex manifolds, we will not discuss them anymore.

2.3   Riemannian Manifolds and Riemannian Metric

Let us go back to $\mathcal{C}^\infty$ differentiable manifolds. From now on, when we talk about differentiable manifolds, we mean $\mathcal{C}^\infty$ differentiable.

Let X be a differentiable manifold of dimension m, and for convenience, suppose that X is embedded in $\mathbb{R}^n$. Let $p \in X$ be a point. Let $\gamma_1, \gamma_2, \ldots, \gamma_m \colon \mathbb{R} \to X$ be paths such that $\gamma_1(t_1) = \gamma_2(t_2) = \cdots = \gamma_m(t_m) = p$ for some $t_1, t_2, \ldots, t_m \in \mathbb{R}$. We can differentiate these

paths to get m tangent vectors $\gamma'_1(t_1), \gamma'_2(t_2), \ldots, \gamma'_m(t_m)$, and if the m tangent vectors are

linearly independent, then their span is called the *tangent space* of X at point p. We will

denote this vector space by T_pX. See [2] for a more general definition of the tangent space

that does not require an embedding into $\mathbb{R}^n$. Since the tangent space is a vector space, we

can assign an inner product to this vector space, and this will give a metric on X.

Definition 2.3.1. A *Riemannian metric* on X is an assignment of an inner product to

each tangent space such that for all $\mathcal{C}^\infty$ paths $\gamma\colon \mathbb{R} \to X$, we have that $\langle \gamma'(t), \gamma'(t) \rangle$ is a

$\mathcal{C}^\infty$ function of t. △

Definition 2.3.2. A *Riemannian manifold* is a differentiable manifold with a Riemannian

metric on it. △

We care about Riemannian 2-manifolds, also known as Riemannian surfaces. To avoid

confusion between Riemann surfaces and Riemannian surfaces, we will refer to Riemannian

surfaces as *metric surfaces* from now on.

With an inner product, we are now able to say many things about paths on X. For

example, when two paths on a manifold intersect, we can find the angle between them on

the manifold. We can also find lengths of paths on a manifold. Paths are that of particular

importance are ones that try to minimize distance. This is a generalization of how a

straight line in the Euclidean plane is the shortest path between two points.

Definition 2.3.3. Let X be a metric surface. Let $\gamma(t)$ be a $\mathcal{C}^\infty$ path. The *length* of a path

$\gamma(t)$ for $t \in (a, b)$ is defined as

$$\int_a^b \sqrt{\langle \gamma'(t), \gamma'(t) \rangle}\ \mathrm{d}t.$$

△

We can now define the distance between two points.

Definition 2.3.4. Let X be a metric surface. Let p, q be points on X. The *distance* between two points p, q is defined as

$$d(p, q) = \inf_{\gamma} \int_a^b \sqrt{\langle \gamma'(t), \gamma'(t) \rangle} \, \mathrm{d}t.$$

$\triangle$

We can now define a geodesic, with the basic idea that it is the path that locally minimizes distance traveled.

Definition 2.3.5. A *geodesic* is a path on a metric surface such that for any two points p, q on the path, the following property is satisfied. For every t, there exists an $\epsilon > 0$ such that for every $u, v \in (t - \epsilon, t + \epsilon)$, we have that $d(\gamma(u), \gamma(v)) = |u - v|$. $\triangle$

We end by talking about maps between two metric surfaces which preserve distances in some way.

Definition 2.3.6. Let X and Y be metric surfaces. A function $F \colon X \to Y$ is an *isometry* if $d(F(p_1), F(p_2)) = d(p_1, p_2)$ for all $p_1, p_2 \in X$. $\triangle$

Definition 2.3.7. Let X and Y be metric surfaces. A function $F \colon X \to Y$ is a *similarity* if there exists a constant $c > 0$ such that for all $p_1, p_2 \in X$, $d(F(p_1), F(p_2)) = c \cdot d(p_1, p_2)$ for all $p_1, p_2 \in X$. $\triangle$

2.4 Covering Spaces

We shall talk about covering spaces, as covered in [9]. Though covering spaces are a topic of algebraic topology, it provides a geometry meaning to fundamental groups. The idea of covering spaces is to take one space and project another onto it, in the style of a "stack of pancakes". We make this precise in the definition.

Definition 2.4.1. A *covering map* is a map $p\colon \widetilde{X} \to X$ such that for every open set $U \in X$, the set $p^{-1}(U)$ is a disjoint union of open sets in $\widetilde{X}$, each of which is homeomorphic to U. △

Definition 2.4.2. A *covering space* of a space X is a space $\widetilde{X}$ with a covering map $p\colon \widetilde{X} \to X$. △

Example 2.4.3. Every space covers itself trivially. ◇

Example 2.4.4. The function $f\colon \mathbb{R} \to S^1$ defined by $f(x) = (\cos 2\pi x, \sin 2\pi x)$ is a covering space from the real line to the circle. ◇

Example 2.4.5. Let $S^1 \subset \mathbb{C}$ be the unit circle. Define $f\colon S^1 \to S^1$ by $f(z) = z^n$ for $n \in \mathbb{N}$. Then f is also a covering space. ◇

Example 2.4.6. Let the helicold be defined as $f(u, v) = (u \cos v, u \sin v, v)$ for $(u, v) \in (0, \infty) \times \mathbb{R}$. This projects the helicold on top of $\mathbb{R}^2 \setminus \{0\}$ by $p(x, y, z) = (x, y)$. This defines a covering space on $\mathbb{R} \setminus \{0\}$. ◇

Let us note two things about the covering space of S^1. There exists several covers of the circle. For example, in both 2.4.4 and 2.4.5, we get that both $\mathbb{R}$ and S^1 can cover S^1 in a nontrivial way. We want to give special treatment to a cover that is maximal in some sense. This is where we get the universal cover.

Definition 2.4.7. A covering space is the *universal cover* if it is simply connected. △

Example 2.4.8. The universal cover of S^1 is $\mathbb{R}$ for it is simply connected. Note that S^1 is not simply connected, so S^1 is not a universal cover of itself. ◇

We now mention why the universal cover is special.

Theorem 2.4.9. *The universal cover $\widetilde{X}$ of a space X covers all connected covers of the space X.*

Definition 2.4.10. Let $p_1 \colon \widetilde{X}_1 \to X$ and $p_2 \colon \widetilde{X}_2 \to X$ be covering spaces. Two covering spaces are *isomorphic* if there exists a homeomorphism $f \colon \widetilde{X}_1 \to \widetilde{X}_2$ such that $p_1 = p_2 \circ f$. △

We now move to automorphisms of covering spaces.

Definition 2.4.11. An automorphism of a covering space is called a *deck transformation*, that is, given a covering map $p \colon \widetilde{X} \to X$, a deck transformation of p is a homeomorphism $f \colon \widetilde{X} \to \widetilde{X}$ such that $p = p \circ f$. △

Example 2.4.12. Let $p \colon \mathbb{R} \to S^1$ be the helix covering space in example 2.4.4. The deck transformations are the ones that vertically shift the helix up and down. Thus, the automorphism group is isomorphic to $\mathbb{Z}$. ◇

Example 2.4.13. Let $p \colon S^1 \to S^1$ be the covering space in example 2.4.5. The deck transformations are rotations of the circle by angles of $2\pi/n$. Thus, the automorphism group is isomorphic to $\mathbb{Z}_n$. ◇

A covering space $p \colon \widetilde{X} \to X$ is called *normal* if for each $x \in X$, and $\widetilde{x}_1, \widetilde{x}_2 \in \widetilde{X}$ where $p(\widetilde{x}_1) = p(\widetilde{x}_2) = x$, there exists a deck transformation that maps $\widetilde{x}_1$ to $\widetilde{x}_2$. A normal covering space is also called *regular*.

Example 2.4.14. Both $p \colon \mathbb{R} \to S^1$ and $p \colon S^1 \to S^1$ are normal covering spaces. ◇

The group of deck transformations acting on covering spaces is just a special case of groups acting on spaces in general. We will now talk about general group actions on topological spaces.

Definition 2.4.15. Let G be a group. Let Y be a topological space. A *group action* of G on Y is a homomorphism $\phi \colon G \to \mathrm{Homeo}(Y)$, where $\mathrm{Homeo}(Y)$ is the group of all homeomorphisms $Y \to Y$. △

Definition 2.4.16. An action is *properly discontinuous* if for every point $x \in X$, there exists a neighborhood U of x such that $U \cap g(U)$ is empty for all but finitely many $g \in G$. $\triangle$

Definition 2.4.17. Let $g \in G$. A *fixed point* for g is a point $y \in Y$ such that $g(y) = y$. $\triangle$

Definition 2.4.18. An action is *free* if every non-identity element of G has no fixed points. $\triangle$

Proposition 2.4.19. *An action is free and properly discontinuous if and only if for each $y \in Y$, there exists a neighborhood U of y such that $g(U)$ are disjoint open sets.*

Given an action of a group G on a space Y, we can form the space Y/G, which is the quotient space of Y where each point $y \in Y$ is identified with all of its images $g(y)$ for all $g \in G$. The points of Y/G are orbits of $Gy = \{g(y) \mid g \in G\}$ in Y and the space Y/G is called the *orbit space* of the action.

Proposition 2.4.20. *Let Y be a path-connected, locally path-connected, and simply connected space. If an action of a group G on a space Y is free and properly discontinuous, then:*

- *The quotient map $p\colon Y \to Y/G$ by $p(y) = Gy$ is a normal covering space.*

- *G is the group of deck transformations of this covering space $Y \to Y/G$.*

- *G is isomorphic to $\pi_1(Y/G)$.*

2.5   Maps between Riemann Surfaces and Branch Points

In this section, we will return to Riemann surfaces and talk about maps between two Riemann surfaces, as discussed in [16].

Definition 2.5.1. Let S_1, S_2 be Riemann surfaces. A function $f\colon S_1 \to S_2$ is *holomorphic* at p if there exist charts $\phi_1\colon U_1 \to V_1$ on S_1 with $p \in U_1$ and $\phi_2\colon U_2 \to V_2$ on S_2 with

$f(p) \in U_2$ such that $\phi_2 \circ f \circ \phi_1^{-1}$ is holomorphic at $\phi_1(p)$. In particular, f is a *holomorphic map* if f is holomorphic for every point of S_1. $\triangle$

Definition 2.5.2. A map $f \colon S_1 \to S_2$ is *biholomorphic* if f is a bijective holomorphic map, and f^{-1} is also a holomorphic map. $\triangle$

Definition 2.5.3. A map $f \colon S_1 \to S_2$ is *anti-biholomorphic* if f is a bijective anti-holomorphic map, and f^{-1} is also an anti-holomorphic map. $\triangle$

Example 2.5.4. The upper half-plane $\mathbb{H}$ and the unit disc $\mathbb{D}$ are biholomorphic as $f \colon \mathbb{H} \to \mathbb{D}$ by $f(z) = \frac{z-i}{z+i}$ is a biholomorphism. $\diamond$

Proposition 2.5.5 (Discreteness of Preimages)**.** *Let $f \colon S_1 \to S_2$ be a non-constant holomorphic map between Riemann surfaces. Then for every $y \in Y$, the preimage $f^{-1}(y)$ is a discrete subset of S_1. If S_1 and S_2 are compact, then $f^{-1}(y)$ is a nonempty finite set for every $y \in Y$.*

We note an important statement that a holomorphic map between two Riemann surfaces locally looks like a power map. In other words, a holomorphic map is very well behaved.

Proposition 2.5.6 (Local Normal Form)**.** *Let $F \colon X \to Y$ be a non-constant holomorphic map defined at $p \in X$. Then there exists a unique integer $m \geq 1$ such that for every chart $\phi_2 \colon U_2 \to V_2$ on Y centered at $F(p)$, there exists a chart $\phi_1 \colon U_1 \to V_1$ on X centered at p such that $\phi_2(F(\phi_1^{-1}(z))) = z^m$.*

Definition 2.5.7. The *multiplicity* of F at p, known as $\mathrm{mult}_p(F)$ is the integer m such that there exists a coordinate map near p and $F(p)$, with $F(z) = z^m$. $\triangle$

Example 2.5.8. Let X be a Riemann surface holomorphic to $\mathbb{C}$. Let $\phi \colon U \to V$ be a coordinate chart for X. Then ϕ has multiplicity 1 for every point of U. $\diamond$

Note that $\mathrm{mult}_p(F)$ is always greater than or equal to 1.

Definition 2.5.9. Let f be a holomorphic map. The point p is a *ramification point* of f if $\text{mult}_p(f) \geq 2$. The point $f(p)$ is called a *branch point*. $\triangle$

Proposition 2.5.10. *Let S_1, S_2 be compact Riemann surfaces. Let $f\colon S_1 \to S_2$ be a holomorphic map. The number of ramification points is finite.*

Definition 2.5.11. A *branched cover* (of the Riemann sphere) is a pair (X, f) where X is a closed Riemann surface and f is a non-constant holomorphic map from S to the Riemann sphere. $\triangle$

While branched covers need not necessarily be over the Riemann sphere, for our purposes, we only care about branched covers over the Riemann sphere, so that is enough. We will now mention why it is called branched cover.

Proposition 2.5.12. *Let (X, f) be a branched cover, where $f\colon X \to Y$. Let $f^*\colon X^* \to Y^*$ be the function where Y^* is Y without the branch points and X^* is the preimage of Y^*. Then f^* is a covering space.*

A proof of this can be found in [7]. One way of viewing branched cover is that it is a covering space in the topological sense except at certain points. There are, though, are finitely many of these points, and these points are well behaved.

2.6 Classification of Surfaces

In this section, we will talk about two classification theorems. The first is for closed topological surfaces; the second is for simply-connected Riemann surfaces. The classification for topological surfaces allows us to define genus, as well as know exactly the surface that we embed on when we try to embed adinkras onto surfaces. The information on classification of topological surfaces can also be found in [14].

We first begin by forming a notion of how to create a new surface from two other surfaces. Simply put, when we want to connect two surfaces, we cut out a disc in each

surface and glue the remaining surfaces together along the hole. This will be made precise in the definition.

Definition 2.6.1. Let S_1 and S_2 be two disjoint surfaces. Let $D_1 \subset S_1, D_2 \subset S_2$ be closed discs. Let $S_1' = S_1 \smallsetminus D_1, S_2' = S_2 \smallsetminus D_2$. A *connected sum* $S_1 \# S_2$ is the quotient space of $S_1' \cup S_2'$ obtained from identifying the boundary of D_1 to D_2. $\triangle$

Lemma 2.6.2. *The topological type of $S_1 \# S_2$ does not depend on the choice of D_1, D_2, nor on the choice of homeomorphisms between their boundaries.*

Example 2.6.3. An n-holed torus is a connected sum of n tori. $\diamondsuit$

Example 2.6.4. The Klein bottle is a connected sum of two projective planes. $\diamondsuit$

Now we need to talk about orientability.

Definition 2.6.5. Let $\mathcal{A}$ be an atlas for the surface S. An atlas is an *oriented atlas* if the determinant of the derivative matrix $\det(\mathrm{d}(\phi_2 \circ \phi_1^{-1}(p)))$ is greater than 0 for all $\phi_1, \phi_2 \in \mathcal{A}$ and for all p. A surface together with an oriented atlas is called an *oriented surface*. $\triangle$

Definition 2.6.6. Let S_1, S_2 be oriented surfaces. Let ϕ be a chart for S_1, and let ψ be a chart for S_2. A map $f \colon S_1 \to S_2$ is *orientation-preserving* if $\det(\mathrm{d}(\psi \circ f \circ \phi^{-1})(p)) > 0$ for all p. A map $g \colon S_1 \to S_2$ is *orientation-reversing* if $\det(\mathrm{d}(\psi \circ g \circ \phi^{-1})(p)) < 0$ for all p. $\triangle$

We can now talk about the classification of closed surfaces.

Theorem 2.6.7 (Classification of Closed Surfaces)**.** *Any closed surface is homeomorphic to one of the following*

- *The unit sphere,*

- *A connected sum of tori,*

- *A connected sum of projective planes.*

Definition 2.6.8. An orientable surface has *genus n* if it is homeomorphic to a connected sum of *n* tori. △

The classification of closed surfaces is useful, but there are also other classification theorems for other types of manifolds. In particular, Riemann surfaces also have a classification theorem. This is different, for Riemann surfaces require holomorphic charts, and so the extra structure changes what kinds of objects the Riemann surfaces are.

Theorem 2.6.9 (Uniformization Theorem)**.** *Any simply connected Riemann surface is biholomorphic to exactly one of the following*

- *The upper half-plane* $\mathbb{H} = \{z \in \mathbb{C} \mid \mathrm{Im}(z) > 0\}$.

- *The complex plane.*

- *The Riemann sphere.*

A proof of the Uniformization Theorem can be found in [7]. The importance of this theorem will be explained in Chapter 4.

3
Topological Graph Theory

Topological graph theory is the study of graphs embedded on surfaces, which also allows graphs to be studied as a topological space. We are interested in this as we want to embed our adinkras, which are graphs with additional structure, onto surfaces. We shall focus on embeddings onto closed surfaces, and so from now on, we will simply refer to closed surfaces as surfaces.

Adinkras are a structure made up of vertices and edges, and the goal will be to study them after embedding into three dimensional surfaces. We will need a way to link adinkras and surfaces in a meaningful way.

3.1   Euler Characteristic

In order to relate graphs, which are structures made up of vertices and edges, and surfaces, which are effectively objects that resemble the plane, we will need to deal with topological invariants related to both and try to link them together. We begin by talking about the Euler characteristic. This information can also be found in [14].

Definition 3.1.1. The *Euler characteristic*, denoted by χ, is the value

$$V - E + F,$$

where V is the number of vertices, E is the number of edges and F is the number of faces. $\triangle$

Name	Vertices	Edges	Faces	Euler Characteristic
Tetrahedron	4	6	4	2
Cube	8	12	6	2
Octahedron	6	12	8	2
Dodecahedron	20	30	12	2
Icosahedron	12	30	20	2

Example 3.1.2. All of the Platonic Solids have Euler characteristic of 2. $\Diamond$

For a polyhedron, calculating this value is straightforward, for the vertices, edges and faces are intuitively clear. However, this can not be directly applied to a smooth surface, such as a sphere, which obviously does not have a clear notion of vertices and edges.

For a simple graph, including adinkras, the only trouble in calculating the Euler characteristic comes from the faces. The faces for a graph will be defined as any cycle that starts and ends at the same vertex. There will be issues with this, such as whether or not we can allow overlapping faces, and generally how to make this precise. Regardless, the Euler characteristic is very simple yet also very useful.

In order to be able to calculate the Euler characteristic for surfaces, we must realize that any surface can be polygonized, meaning that it can be turned into a polyhedron.
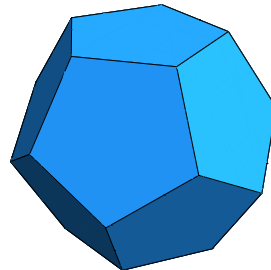

Figure 3.1.1: A dodecahedron has 20 vertices, 30 edges, and 12 faces, so $\chi = 2$.

Another topological invariant of surfaces is the genus of a surface. Recall that formally, the genus of a surface is n if it is homeomorphic to a connected sum of n tori. While we have formally classified the genus of all surfaces, a more intuitively way of viewing genus is seeing it as the number of "handles" that a surface has. This is a much better invariant to work with for surfaces than the Euler characteristic, for the genus, in many cases, can be immediately figured out. Another important property is that the genus is connected to the Euler characteristic in the following proposition.

Proposition 3.1.3. *The Euler characteristic and the genus are related by the following formula:*

$$\chi = 2 - 2g,$$

where χ is the Euler characteristic and g is the genus.

Relating the genus of a surface to the Euler characteristic gives us a very important result. Any polygonization of the surface always results in the same Euler characteristic. Thus, an embedding of a graph onto a surface can be viewed as a form of polygonization, and we are able to relate graphs and surfaces as a result.
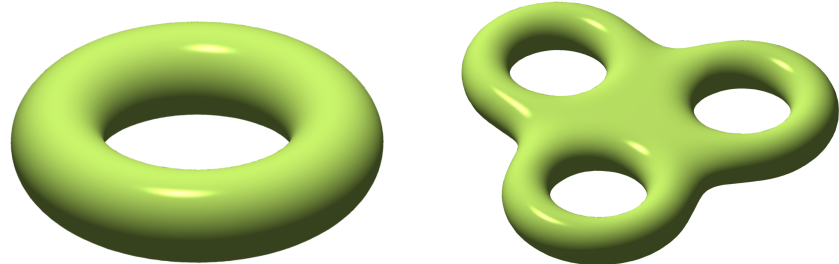

Figure 3.1.2: Two tori. The left torus has a genus of 1. The right triple torus has a genus of 3.

3.2 Graph Embeddings and Ribbon Graphs

Now that we have found a way to find the surfaces that graphs embed on, we can now talk about how these graphs and surfaces can be connected. This information can also be found in [8]. We begin by defining a graph embedding, which is very easy to do as it is simply a map from a graph to a surface.

Definition 3.2.1. Let G be a graph. Let S be a surface. A function $i\colon G \to S$ is an *embedding* if i is continuous and injective. $\triangle$

If we view the graph G as a subset of the surface S, we have that an embedding is the inclusion map.

Definition 3.2.2. A *2-cell embedding* is an embedding where $S \smallsetminus G$ is the union of discs. $\triangle$

It turns out that what we need for a graph embedding is a list of permutations of the edges attached to each vertex for every vertex.

Definition 3.2.3. Let G be a connected finite graph. A *ribbon structure* $O = \{\pi_v \mid v \in V(G)\}$ is a set of permutations such that for each vertex $v \in V(G)$, there is a cyclic permutation π_v of the edges connected to v. A *ribbon graph* (G, O) is a graph with a ribbon structure. Ribbon structures are also known as *rotation systems*. We consider the permutation π_v as the counterclockwise order on the vertex. $\triangle$

Let $i_1\colon G \to S_1$ and $i_2\colon G \to S_2$ be embeddings. These two embeddings are equivalent if there exists an orientation-preserving homeomorphism $h\colon S_1 \to S_2$ such that $h \circ i_1 = i_2$.

Theorem 3.2.4. *Every ribbon structure induces a unique embedding of G onto an oriented surface. Every embedding of a graph G into an oriented surface induces a unique ribbon structure for G.*

Now all we need is how to take the ribbon graph and create the faces out of it. The following algorithm describes how we get the faces.

Algorithm 3.2.5 (Face Tracing Algorithm)**.** Let G be a graph. Choose initial vertex v_0 of G and first edge e_1. The boundary walk begins at v_0 and goes along e_1. Let v_1 be the other endpoint of e_1. The second edge e_2 in the boundary walk is the edge after e_1 at v_1. In general, if the walk traced so far ends with edge e_i at vertex v_i, then the next edge e_{i+1} is the edge after e_i at v_i. The boundary walk is finished at edge e_n if the next two edges are e_1 and e_2. Then to start a different boundary walk, begin at the second edge of any corner that does not appear in any previously traced faces. If there are no unused corners, then all faces have been traced. ◇

Note that the boundary walks do not necessarily stop when the first edge e_1 is encountered for a second time, as we might be on a different side of e_1. The way to figure out if we are indeed on the same side is by following up e_1 with e_2.

3.3   Dessins d'Enfants and Belyi Pairs

Dessins d'enfants, French for children's drawings, are a type of graph that provides connections to Riemann surfaces, as well as to algebraic geometry. We shall first define what dessins d'enfants are and then show how they are connected to Riemann surfaces. From there, we shall show how adinkras are related to dessins d'enfants. Proofs in this sections are from [7] unless otherwise noted.

Definition 3.3.1. Let X be an oriented compact topological surface. Let $D \subset X$ be a finite graph embedded on X. We say that the pair (X, D) is a *dessin d'enfant*, or dessin for short, if

- D is connected,

- D is bipartite,

- $X \smallsetminus D$ is the union of finitely many topological discs, called the *faces* of D.

Two dessins $(X_1, D_1), (X_2, D_2)$ are *equivalent* if there exists an orientation preserving homeomorphism $\phi \colon X_1 \to X_2$ such that $\phi|_{D_1}$ is an isomorphism from D_1 to D_2. $\quad\triangle$
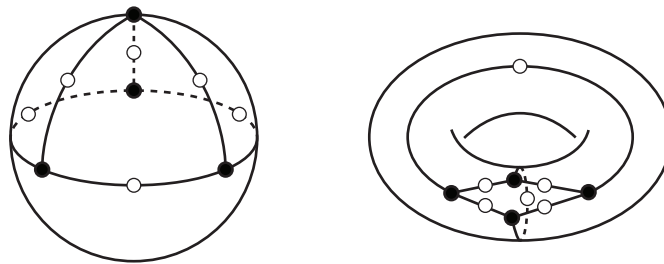

Figure 3.3.1: Two different dessins d'enfants. The two graphs are the same, but since they are embedded in different surfaces, they are different dessin d'enfants.

Example 3.3.2. The figure 3.3.1 shows two different dessins d'enfants. Both have the same graph, but one is embedded on a sphere, and the other is embedded on a torus. $\quad\lozenge$

Example 3.3.3. The platonic solids can be made into dessins. Though the graphs of platonic solids are not bipartite, we can force them to be bipartite. Let the vertices of a platonic solid be the *black* vertices. For every edge, we separate the edge in the middle with a *white* vertex. The sets of black vertices and white vertices form a bipartition. In fact, every non-bipartite graph can be made bipartite this way. $\quad\lozenge$

In example 3.3.3, we described a way to take any graph and construct a new bipartite graph out of it that is essentially the same. Thus, dessins d'enfants can apply to any graph.

What makes dessins interesting is that they can be related to Riemann surfaces. We are always able to find a complex structure associated to the surface of any dessin. In order to do that, we will talk about Belyi functions.

Definition 3.3.4. Let S be a closed Riemann surface. A *Belyi function* is a holomorphic function $f\colon S \to \widehat{\mathbb{C}}$, with branch points $\{0, 1, \infty\}$.   △

We note that a Belyi function has exactly three branch points. This choice is intentional, as any function with less than three branch points are all isomorphisms of the Riemann sphere, as will be discussed below.

For the case with no branch points, note that f is an unramified function, so f is an isomorphism of the Riemann sphere. For the case with one branch point, note that $f\colon S \smallsetminus f^{-1}(\infty) \to \widehat{\mathbb{C}} \smallsetminus \{\infty\}$ is an isomorphism, so f is an isomorphism of the Riemann sphere. For the case with two branch points, note that $f\colon S \smallsetminus \{0, \infty\} \to \widehat{\mathbb{C}} \smallsetminus \{0, \infty\}$ is an isomorphism, so f is once again an isomorphism of the Riemann sphere.

Definition 3.3.5. A *Belyi pair* (X, f) is a pair where X is a compact Riemann surface and $f\colon X \to \widehat{\mathbb{C}}$ is a Belyi function.   △

Definition 3.3.6. Two Belyi pairs $(X_1, f_1), (X_2, f_2)$ are *equivalent* if they are equivalent as ramified coverings, i.e., if there exists a biholomorphism $h\colon X_1 \to X_2$ such that $f_1 = f_2 \circ h$.   △

We will now relate Belyi pairs and dessins d'enfants. Let (S, f) be a Belyi pair, and define a graph D_f as follows:

1. Let $f^{-1}(0)$ be white vertices and $f^{-1}(1)$ be black vertices.

2. The edges of components of the $f^{-1}((0, 1))$, where $(0, 1)$ denotes the open interval from 0 to 1.

We consider the set $D_f = f^{-1}([0, 1])$, the set of preimages of the line segment from 0 to 1. From theorem 1.74 of [7], we are able to conclude that $f^{-1}(\widehat{\mathbb{C}}) \smallsetminus [0, 1]$ is a disjoint union of discs, and its complement is a connected graph. Thus, from any Belyi pair, we can find a dessin d'enfant associated to it. It is also possible to go in the opposite direction:

Theorem 3.3.7 (Grothendieck Correspondence)**.** *There is a one to one correspondence between the equivalence classes of dessins and equivalent classes of Belyi pairs.*

More precisely, let $(X_1, f_1), (X_2, f_2)$ *be Belyi pairs, and let* $(X_1, D_1), (X_2, D_2)$ *be the corresponding dessins, respectively. Then for any equivalence* $h\colon (X_1, D_1) \to (X_2, D_2)$, *there exists an equivalence* $\phi\colon (X_1, f) \to (X_2, f_2)$ *that induces the same homeomorphism of* D_1 *to* D_2.

Corollary 3.3.8. *Let* (X, f) *be a Belyi pair, and let* (X, D) *be the corresponding dessin. Then for any self-equivalence* $h\colon (X, D) \to (X, D)$, *there exists a self-equivalence* $\phi\colon (X, f) \to (X, f)$ *that induces the same automorphism of* D.

We note that equivalences of dessins preserve orientation. This is too restrictive, as we need to consider automorphisms that reverse orientation, so we have a construction that allows us to do that.

Definition 3.3.9. Two dessins $(X_1, D_1), (X_2, D_2)$ are *anti-equivalent* if there exists an orientation-reversing homeomorphism $\phi\colon X_1 \to X_2$ such that $\phi|_{D_1}$ is an isomorphism from D_1 to D_2. $\triangle$

Theorem 3.3.10. *Let* (X, f) *be a Belyi pair. Let* (X, D) *be the corresponding dessin. Then for any anti-equivalence* $h\colon (X, D) \to (X, D)$, *there exists an anti-equivalence* $\phi\colon (X, f) \to (X, f)$ *that induces the same automorphism of* D.

Proof. Let (X, f) be a Belyi pair. Let X^* be the oriented surface obtained from X by switching the orientation. Let $\overline{f}(x) = f(\overline{x})$. Then $(X^*, \overline{f})$ is also a Belyi pair. Then let $h\colon (X, D) \to (X^*, D)$ be an equivalence of dessins. Then we get an equivalence $\phi\colon (X, f) \to (X^*, \overline{f})$ that induces an automorphism of D, and so ϕ is an anti-equivalence from (X, f) to (X, f) $\square$

We will now show that more generally, dessins are in one to one correspondence with ribbon graphs.

Proposition 3.3.11. *Equivalence classes of dessin d'enfants are in one to one correspondence to equivalence classes of bipartite connected ribbon graphs.*

Proof. Let (X, D) be a dessin d'enfant. Let V be the set of vertices for D. Let $v \in V$ and let $U \subset X$ be a neighborhood of v. Let $p_v \colon [0, 1] \to U$ be a positively oriented path surrounding v. This path defines a cyclic ordering of the edges attached to v. We can do this for each $v \in V$, so we get a ribbon structure. Thus, D is a ribbon graph.

Let D be a bipartite ribbon graph. From the face tracing algorithm 3.2.5, we can attach 2-cells to the ribbon graph to create a topological surface X. The 2-cells we attached are disjoint, so (X, D) is a dessin d'enfant. $\square$

In summary, we have shown that there exist one to one correspondences between the following:

- Belyi pairs,

- Dessins d'enfants,

- Ribbon graphs.

3.4   Adinkras and Rainbows

Let us go back to adinkras. Like all graphs, adinkras have a clear notion of vertices and edges, but the faces are not immediately clear. However, we need find a canonically way to form faces in order to calculate the Euler characteristic. This is where we bring back the concept of the rainbow. The definition will be repeated here again.

Definition 3.4.1. A *rainbow* is a cyclic ordering of the edge colors of a chromotopology.

$\triangle$

Adinkras with a rainbow can be given the structure of a ribbon graph where all of the white vertices have the counterclockwise permutation order of the rainbow, and the black vertices have permutation in the clockwise permutation order of the rainbow. This is important as we will show in the following proposition.

Proposition 3.4.2. *For an embedding of an adinkra on a surface, all faces are quadrilaterals whose edges are two adjacent colors from the rainbow.*

Proof. We shall use the face tracing algorithm 3.2.5. We start at a white vertex v_1, and walk an on edge e_i to arrive at a black vertex v_2. We go to the next edge, which is e_{i-1}. Then we walk on that edge to arrive at second white vertex v_3. The next edge is e_i, so we walk to a second black vertex v_4. The next edge in the permutation is e_{i-1}, so we follow that edge back to the first white vertex v_1. This is because one property of the adinkra is that 2 colored edges form 4-cycles. We walked on each of the edges e_{i-1} and e_i twice, so we must have returned back to our original vertex. Since this is a 4-cycle, the face attached is a quadrilateral. $\square$

As a result of assigning a rainbow to an adinkra, we get that an adinkra is also ribbon graph. By proposition 3.3.11, we get that adinkras with a rainbow assigned are in fact dessins d'enfants. Then by proposition 3.3.7, treating adinkras with a rainbow assigned as a dessin d'enfant corresponds to a Belyi pair. Thus, we are able to get a complex structure from adinkras embeddings into a surface. So in fact, adinkras embed onto Riemann surfaces.

Example 3.4.3. The $n = 3, N = 4$ adinkra embeds onto a torus, as shown in figure 3.4.1. Let the edge colors be red, blue, green, pink. The rainbow is the order in which the edge colors were given. Using the rainbow, we look at the 4-cycles formed by the following combinations: (red blue), (blue green), (green pink), (pink red). We attach 2-cells to every 4-cycle whose edges are those color combinations. Doing this correctly, we attach 8 faces
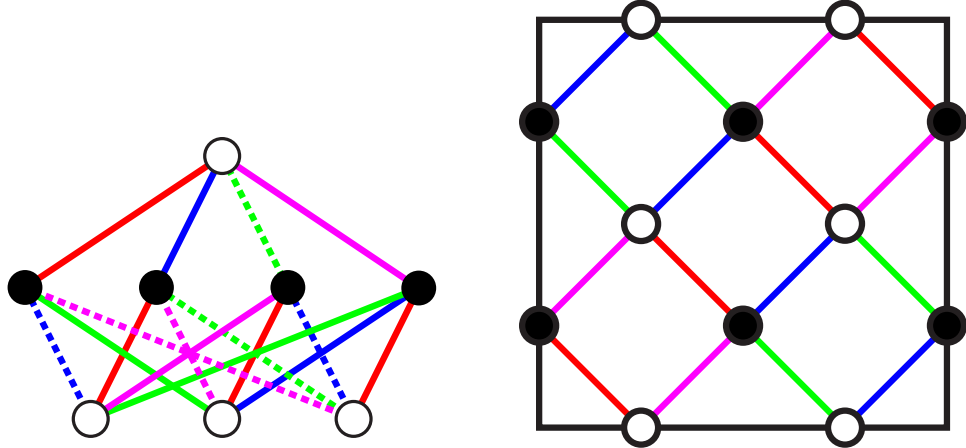
Figure 3.4.1: The adinkra with $K_{4,4}$ topology, and its embedding into a torus.

to form a torus. Note that the following combinations are not considered: (red green), (blue pink). ◊

Proposition 3.4.4. *For an adinkra with 2^n vertices and degree N, the Euler characteristic and genus is*

$$\chi = 2^n \left(1 - \frac{N}{4} \right),$$
$$g = 1 - 2^{n-1} \left(1 - \frac{N}{4} \right).$$

Proof. From proposition 3.1.3, we have the relationship $2 - 2g = V - E + F$. We note that the choice of rainbow for an adinkra does not change the number of faces.

We note that the number of vertices in an adinkra is 2^n, where $n \leq N$, and that there are N edges attached to each vertex. Thus, we have the following,

$$V = 2^n,$$
$$E = V(N/2) = 2^n \left(\frac{N}{2} \right) = 2^{n-1} N,$$
$$F = V(N/4) = 2^n \left(\frac{N}{2^2} \right) = 2^{n-2} N.$$

n	N	Vertices	Edges	Faces	Genus	χ
2	2	4	4	2	0	2
3	3	8	12	6	0	2
3	4	8	16	8	1	0
4	4	16	32	16	1	0
4	5	16	40	20	3	-4
5	5	32	80	40	5	-8
4	6	16	48	24	5	-8
5	6	32	96	48	9	-16
6	6	64	192	96	17	-32

Table 3.4.1: A table of low dimensional adinkras, their degrees, number of vertices, number of edges, and isomorphism type.

Finally, using these numbers, we can calculate that the Euler characteristic is

$$\chi = 2^n - 2^{n-1}N + 2^{n-2}N$$
$$= 2^n \left(1 - \frac{N}{4} \right).$$

The genus is

$$g = 1 - 2^{n-1} \left(1 - \frac{N}{4} \right).$$

$\square$

Now we will list a few examples of adinkras and their genus.

Example 3.4.5. The cube adinkra has 8 vertices, 12 edges, and 6 faces. Thus, as expected from its name, has Euler characteristic of 2, matching that of a cube. $\Diamond$

Example 3.4.6. The cube adinkra with antipodal edges attached, or the adinkra with $K_{4,4}$ topology, has 8 vertices, 16 edges, and 8 faces, so it has Euler characteristic of 0. This matches the Euler characteristic of a torus of genus 1. Note that without a rainbow, if we attach every single possible face to every two color 4-cycle, we end up attaching $2\binom{4}{2} = 12$ faces. $\Diamond$

4

Non-Euclidean Geometry

When we unfold a torus into a quadrilateral, we get four corners, and the sum of the interior angles is 2π. The four corners must glue to the same point, and all of the angles sum to 2π. However, there are problems when we deal with surfaces with genus greater than 1. For example, a two-holed torus unfolds into an octagon. The interior angles sum to 6π. The eight corners all glue to a single point. This is an issue because in the Euclidean plane, all of the angles have enough space sum to 2π, but they sum up to three times that amount, making such a gluing impossible. This is the motivation for us to learn about *hyperbolic geometry.* More information on hyperbolic geometry can also be found in [3].

4.1 Description

In Euclidean geometry, there exist Euclid's postulates, one of which is the parallel postulate. The parallel postulate states that given a point P and a line L, there exists a unique line X that contains P and never intersects L. Mathematicians tried for a very long time to use Euclid's other postulates to prove the parallel postulate but failed. They eventually proved that the parallel postulate is necessary for Euclidean space by creating

other geometric spaces that satisfy all of Euclid's postulates except the parallel postulate. But before we talk about such spaces, we need to extend the notion of "straight" to more general spaces. We will focus on the property that a straight line in Euclidean space is the shortest distance between two points. Recall that we defined a geodesic in section 2.3 formally. What that definition is trying to say is that a *geodesic* is the path between two points that travels the least amount of distance.

Example 4.1.1. The geodesics in Euclidean space are straight lines. $\Diamond$

One such geometry where the parallel postulate does not hold true is spherical geometry. This is the geometry on the surface of a sphere. The shortest path between two points is a great circle, so great circles are the geodesics. Thus, given a point P and a geodesic G, any geodesic containing the point must intersect G. Thus, there does not exist a geodesic that contains P and does not intersect G.

Spherical geometry does not satisfy the parallel postulate by having no geodesics that have the desired property, but in doing so, some of Euclid's other postulates are not satisfied. For example, a requirement in Euclidean geometry is that the shortest path between two points is unique. This is not true in spherical geometry, as antipodal points on a sphere have many different great circles containing them. As a result, one can argue that spherical geometry does not prove the requirement of the parallel postulate, as it does not satisfy other postulates as well. In order to prove that the parallel postulate, there exists a geometry where all of Euclid's postulates except the parallel postulate are satisfied. This is known as hyperbolic geometry.

Definition 4.1.2. *Hyperbolic geometry* is the geometry obtained when all of Euclid's postulates are satisfied and the parallel postulate is false. $\triangle$

By the definition of hyperbolic geometry, we receive absolutely no insight to how the space would even look like. Since the observable world appears to be Euclidean, we only

have models that approximate hyperbolic geometry. Two such models are the Poincaré half-plane model, and the Poincaré disc model. These two models are chosen because compared to Euclidean space, they are conformal, meaning that the angles between two geodesics are the same as they appear in Euclidean space.

Definition 4.1.3. Let f be a function. Then f is *conformal* if it preserves angles. $\triangle$

4.2 Upper Half-Plane Model

The upper half-plane model is a model of hyperbolic geometry by taking the upper half of the Cartesian plane and assigning a specific metric on it that allows it to satisfy Euclid's postulates except for the parallel postulate. We do this by considering a metric space with a specific inner product.

Definition 4.2.1. The upper half-plane model is the metric surface

$$\mathbb{H} = \{z \in \mathbb{C} \mid \text{Im}(z) > 0\}$$

with inner product

$$\langle \vec{v}, \vec{w} \rangle = \frac{1}{y^2} \vec{v} \cdot \vec{w}.$$

$\triangle$

Note that the upper half-plane includes all points above the x-axis but does not include the axis itself. The inner product induces a family of geodesics. There are two types of geodesics in this model. One type is vertical rays where the x value is held constant. The other type are semicircles that are orthogonal to the x-axis. Once again, the half-plane model does not include the axis, so the points that would intersect the x-axis are not included.

Proposition 4.2.2. *The geodesics in the upper half-plane model are semi-circular arcs orthogonal to the x-axis and vertical rays.*

Now an important aspect is to talk about how distance works in this model. Since we are given an inner product, we can figure out the distance formula directly. However, it is also useful to see how distance works from an intuitive point of view. The farther away from the x-axis, the less distance appears to have been traveled. Thus, paths that travel shorter distances tend to travel upwards as much as possible.

Proposition 4.2.3. *The metric of the upper half-plane model is given as*

$$d((x_1, y_1), (x_2, y_2)) = \cosh^{-1}\left(1 + \frac{(x_2 - x_1)^2 + (y_1 - y_2)^2}{2y_1 y_2}\right).$$

Finally, to clarify, the metric does not calculate the length of what we see to be a straight line between between two points, but rather the geodesic between two points. In Euclidean space, the geodesic would be straight lines. In the upper half-plane, the geodesic are vertical lines or circular arcs. In order to figure out the distance traveled along a non-geodesic path, we note that this is similar to calculating the arc length. In fact, we use the exact same formula, but the only difference is the choice of the inner product depending on the space we are considering.

4.3   Poincaré Disc Model

Definition 4.3.1. The Poincaré Disc model is the metric surface

$$\mathbb{D} = \{z \in \mathbb{C} \mid |z| < 1\}$$

with the inner product

$$\langle \vec{v}, \vec{w} \rangle = 4 \frac{\vec{v} \cdot \vec{w}}{(1 - x^2 - y^2)^2}.$$

$\triangle$

The Poincaré disc model is another model that helps visualize the hyperbolic plane. Unlike the half-plane model, the disc model is bounded. There are a few consequences.

First, we can observe the plane in its entirety. However, there will be more distortion and it will be harder to work with compared to the half-plane model.

The disc that we choose for the disc model is the unit disc. Like the half-plane model, we do not include the boundary. Geodesics are circular arcs that are orthogonal to the boundary circle. Another type of geodesic are lines that appear to be straight, but this only occurs if the geodesic passes through the center of the unit disc.

Proposition 4.3.2. *The geodesics of the Poincaré disc model are circular arcs orthogonal to the boundary and diameters.*

Straight-line geodesics can be viewed as a deformed circular arc, where the radius is infinity; the same could be said in the half-plane model as well.

We will now relate the two models of the hyperbolic plane.

Proposition 4.3.3. *The upper half-plane model of hyperbolic geometry and the Poincaré disc model of hyperbolic geometry are conformal.*

4.4 Triangles and Calculations

Triangles are the most basic polygons in the Euclidean plane, and by studying them well, we can extend them to other polygons quite easily. That is why it is most useful to have the a strong understanding of triangles in the hyperbolic plane.

In Euclidean geometry, we have the regular trigonometric functions, which are based on the unit circle. There also exist hyperbolic trigonometric functions. There are two ways to view the hyperbolic trigonometric functions. One way is to view them as based on a unit hyperbola in Euclidean space. Another way is to view them as an analog to the trigonometric functions in hyperbolic space. Hyperbolic functions play an important role in figuring out calculations of lengths and angles in hyperbolic space.

Definition 4.4.1. The *hyperbolic sine* function is defined as

$$\sinh x = \frac{e^x - e^{-x}}{2}.$$

The *hyperbolic cosine* function is defined as

$$\cosh x = \frac{e^x + e^{-x}}{2}.$$

$\triangle$

Once we have defined these two functions, all other functions follow. For example, the hyperbolic tangent function is defined as the quotient of the hyperbolic sine and hyperbolic cosine functions.

Now that we have a definition of the hyperbolic functions, we can start to form useful identities that can help with calculations. For example, with trigonometric functions, we have that $\sin^2 x + \cos^2 x = 1$. There exists a similar identity with hyperbolic functions as well.

Proposition 4.4.2. *We have the following identity for the hyperbolic functions,*

$$\cosh^2 x - \sinh^2 x = 1.$$

Proof. Observe that

$$\begin{aligned}
\cosh^2 x - \sinh^2 x &= \frac{(e^x + e^{-x})^2}{2^2} - \frac{(e^x - e^{-x})^2}{2^2} \\
&= \frac{e^{2x} + 2 - e^{-2x} - e^{2x} + 2 + e^{-2x}}{4} \\
&= 1.
\end{aligned}$$

This concludes the proof. $\square$

While this identity is fundamental, it does not help for all situations. Just like with trigonometric functions, all other useful identities have a corresponding equivalent, some of which are given below.

Proposition 4.4.3 (Sum of Angles Formula)**.** *The hyperbolic sine and cosine of the sum of two numbers are given as follows,*

$$\sinh(x+y) = \sinh x \cosh y + \sinh y \cosh x$$

$$\cosh(x+y) = \cosh x \cosh y + \sinh x \sinh y.$$

Proposition 4.4.4 (Double Angle Formula)**.** *The hyperbolic sine and cosine of twice of a number are given as follows,*

$$\sinh 2x = 2 \sinh x \cosh x$$

$$\cosh(2x) = \cosh^2 x + \sinh^2 x.$$

Proposition 4.4.5 (Half Angle Formula)**.** *The hyperbolic sine and cosine of half of a number are given as follows,*

$$\sinh \frac{x}{2} = \sqrt{\frac{1}{2}(\cosh x - 1)}$$

$$\cosh \frac{x}{2} = \sqrt{\frac{1}{2}(\cosh x + 1)}$$

The proofs of these propositions can be easily proven using the definitions of the hyperbolic functions.

We shall have one more proposition, this time about the inverse hyperbolic functions.

Proposition 4.4.6. *Let* $\sinh^{-1} x$ *be a function such that* $\sinh(\sinh^{-1} x) = x$. *Let* $\cosh^{-1} x$ *be a function such that* $\cosh(\cosh^{-1} x) = x$. *Then*

$$2 \sinh^{-1} x = \cosh^{-1}(2x^2 + 1),$$

$$2 \cosh^{-1} x = \cosh^{-1}(2x^2 - 1).$$

Proof. Let $y = 2 \sinh^{-1} x$. Then we have that $x = \sinh(y/2)$. We now use the half-angle formula to get that

$$x = \sqrt{\frac{\cosh y - 1}{2}}.$$

Then we solve for y to get that

$$y = \cosh^{-1}(2x^2 + 1),$$

Let $z = 2\cosh^{-1} x$. Then we have that $x = \cosh(z/2)$. We now use the half-angle formula to get that

$$x = \sqrt{\frac{1 + \cosh z}{2}}.$$

Then we solve for z to get that

$$z = \cosh^{-1}(2x^2 - 1),$$

as desired. $\qquad\square$

Recall that in the Euclidean plane, the interior angles of a triangle sum to π. In the hyperbolic plane, the sum of the interior angles of a hyperbolic triangle must sum up to less than π. In fact, the sum of the interior angles of a triangle depends on the area of the triangle.

Proposition 4.4.7. *The sum of the interior angles of a triangle in hyperbolic space is $\pi - A$, where A is the area of the triangle.*

Note that we have a strange relationship between the angles of a triangle and its area. The area of a hyperbolic triangle is given a name for this reason.

Definition 4.4.8. The area of a hyperbolic triangle is the *angular defect* of the triangle.

$\triangle$

In fact, it is even possible to have a triangle whose angles add up to a total of zero. This has a special name.

Definition 4.4.9. A polygon in the hyperbolic plane is called *ideal* if all angles are 0. $\triangle$

One property of the Euclidean plane is that it is *homothetic*, which means that there exists scaling in some form. For example, three angles determine the proportions of the

lengths of all three sides of the triangle in the Euclidean plane. This also means that two triangles in the Euclidean plane where the angles of both triangles have all congruent are similar triangles, but not congruent triangles. However, in the hyperbolic plane, three angles uniquely determine the lengths of all three sides of a triangle.

We will now state an even stronger statement. Suppose we have a regular polygon in the Euclidean plane, and we are given an angle that is less than the interior angle of the regular polygon. Then we can find a regular polygon in the hyperbolic plane with the same number of sides with all of the interior angles being the given angle. We can also conclude that the side lengths will be uniquely determined from the interior angle.

Proposition 4.4.10. *Let θ be an angle such that $\theta < \pi \frac{n-2}{n}$ for some n. Let P be an n-sided regular polygon in the hyperbolic plane with interior angle θ. Then the side lengths of P is uniquely determined.*

Proof. Take P and draw geodesics from the center of P to the vertices of P. Then we have n equivalent isosceles triangles where the three interior angles are $2\pi/n, \theta/2, \theta/2$. Since three angles uniquely determine the side lengths of a hyperbolic triangle, we get that the side length of the regular polygon is uniquely determined. □

We will now talk about special theorems about triangles, such as the Pythagorean theorem. There exist equivalent versions that apply for the hyperbolic plane. These can also be found in [20]. Let the sides of a triangle be a, b, c and the opposite angles be A, B, C. We shall begin with the hyperbolic law of cosines.

Proposition 4.4.11 (Hyperbolic Law of Cosines)**.**

$$\cosh c = \cosh a \cosh b - \sinh a \sinh b \cos C.$$

In the Euclidean case, the law of cosines is a generalization of the Pythagorean theorem. This is also true of the hyperbolic law of cosines as well. For hyperbolic triangles where one of the angles is $\frac{\pi}{2}$, we get the hyperbolic Pythagorean theorem.

Proposition 4.4.12 (Hyperbolic Pythagorean Theorem)**.** *Suppose $C = \pi/2$. Then*

$$\cosh c = \cosh a \cosh b.$$

Finally, we end with an important formula that has no equivalent in Euclidean geometry. This is due to the fact that three angles cannot uniquely determine any side lengths in the Euclidean plane, but three angles do uniquely determine the side lengths in the hyperbolic plane.

Proposition 4.4.13 (Dual Hyperbolic Law of Cosines)**.**

$$\cos C = -\cos A \cos B + \sin A \sin B \cosh c.$$

We will mention that the law of sines also has an equivalent in the hyperbolic plane, but it will not be as useful as compared to the law of cosines.

Proposition 4.4.14 (Hyperbolic Law of Sines)**.**

$$\frac{\sin A}{\sinh a} = \frac{\sin B}{\sinh b} = \frac{\sin C}{\sinh c}$$

With all of these formulas, we can perform calculations in the hyperbolic plane as needed.

4.5   Isometries in the Hyperbolic Plane

In this section, we shall study the isometries of the hyperbolic plane. Recall that isometries are functions that preserve distances. The point of isometries is to provide another way to analyze hyperbolic space. We begin by defining Möbius transformations, and then we

eventually show how it relates to the isometries of the hyperbolic plane. This information

can also be found in [13].

Definition 4.5.1. A *Möbius transformation* is a function $f \colon \mathbb{C} \to \mathbb{C}$ defined as

$$f(z) = \frac{az + b}{cz + d}$$

for $a, b, c, d \in \mathbb{R}$ and $ad - bc = 1$. $\triangle$

We note that the composition of two Möbius transformations is yet again another

Möbius transformation. So indeed, the set of Möbius transformations forms a group under

function composition, and we will denote this by Möb.

Proposition 4.5.2. *The set of Möbius transformations forms a group under function*

composition.

Let $\phi \colon \mathrm{SL}(2, \mathbb{C}) \to$ Möb be a function where

$$\begin{pmatrix} a & b \\ c & d \end{pmatrix} \mapsto \frac{az + b}{cz + d}.$$

It is easy to check that ϕ is a homomorphism. We note that $\ker(\phi) = \{\mathbb{I}_2, -\mathbb{I}_2\}$ where $\mathbb{I}_2$

is the 2×2 identity matrix. By the first isomorphism theorem, we get that

$$\mathrm{SL}(2, \mathbb{C}) / \{\mathbb{I}_2, -\mathbb{I}_2\} = \text{Möb} .$$

We give the quotient a special name, $\mathrm{SL}(2, \mathbb{C}) / \{\mathbb{I}_2, -\mathbb{I}_2\} = \mathrm{PSL}(2, \mathbb{C})$.

Definition 4.5.3. Let $\mathbb{I}_2$ be the 2×2 identity matrix. The *projective linear group* $\mathrm{PSL}(2, \mathbb{C})$

is defined as $\mathrm{SL}(2, \mathbb{C}) / \{\mathbb{I}_2, -\mathbb{I}_2\}$. $\triangle$

Proposition 4.5.4. *In the upper half-plane model, the elements of* $\mathrm{PSL}(2, \mathbb{R})$ *are*

orientation-preserving isometries of the hyperbolic plane. We denote such isometries by

$\mathrm{Isom}_+(\mathbb{H})$. *In other worlds, the orientation-preserving isometries of the upper half-plane*

are $\{x \in \text{Möb} \mid a, b, c, d, \in \mathbb{R}, ad - bc = 1\}$.

It follows from this proposition that the group $\text{Isom}_+(\mathbb{H})$ is isomorphic to $\text{PSL}(2, \mathbb{R})$.

We now want to talk about $\text{Isom}_+(\mathbb{H})$ in a topological manner. First, elements of the group $\text{SL}(2, \mathbb{R})$ can be identified with elements in $\mathbb{R}^4$. More specifically, $\text{SL}(2, \mathbb{R})$ can be identified as the set

$$\{(a, b, c, d) \in \mathbb{R}^4 \mid ad - bc = 1\}.$$

Then $\text{SL}(2, \mathbb{R})$ inherits the topology from $\mathbb{R}^4$, and the group $\text{PSL}(2, \mathbb{R})$ receives the quotient topology as a result.

We will now talk about a specific subset of the isometries of the hyperbolic plane that is more manageable and will lead us to notions that will be useful later.

Definition 4.5.5. A subgroup T of $\text{Isom}_+(\mathbb{H})$ is called *discrete* if the induced topology on T is a discrete topology, i.e., T is a discrete set in the topological space $\text{Isom}_+(\mathbb{H})$. A discrete subgroup of $\text{Isom}_+(\mathbb{H})$ of the hyperbolic plane is called a *Fuchsian group*. △

Example 4.5.6. A compact surface with an atlas of charts that map to the hyperbolic plane is known as a *hyperbolic surface*. Let X be a hyperbolic surface. The universal cover $\widetilde{X}$ of X is isometric with the hyperbolic plane. The deck transformations of the cover are hyperbolic isometries, so they are elements of Möb. We can show that deck transformations are discrete, and as a result, the group of deck transformations is a Fuchsian group. The Fuchsian group is in fact $\pi_1(X)$. ◇

We will now mention one important result that we need Fuchsian groups for.

Definition 4.5.7. Let G be a group that acts properly discontinuously on the metric space X. A closed set $F \subset X$ is a *fundamental region* if it satisfies the following properties:

- $\bigcup_{g \in G} g(F) = X$,

- $F^\circ \cap g(F^\circ) = \emptyset$ for all non-identity $g \in G$, where F° denotes the interior of F.

The family $\{g(F) \mid g \in G\}$ is called the *tessellation* or *tiling* of X. △

Example 4.5.8. A fundamental region of the complex torus $\mathbb{C}/(\mathbb{Z}\oplus\mathbb{Z}i)$ is the closed unit square. $\Diamond$

Definition 4.5.9. Let Γ be an arbitrary Fuchsian group and let $p \in \mathbb{H}$ be not fixed by any non-identity element of Γ. The set

$$D_p(\Gamma) = \{z \in \mathbb{H} \mid d(z,p) \leq d(z,g(p)) \text{ for all } g \in \Gamma\}$$

is called the *Dirichlet region* for Γ centered at p. $\triangle$

We can have the group action generate a tiling of the hyperbolic plane. However, we can start at any tiling and get the group back from it.

Example 4.5.10. In figure 4.5.1, the group of all orientation-preserving isometries of the tiling is isomorphic to $\text{PSL}(2,\mathbb{Z})$.

The group G of color-preserving, orientation-preserving isometries of the tiling has presentation $\langle r, s, t \mid r^2 = s^2 = t^2 = 1 \rangle$ and is an index-three subgroup of $\text{PSL}(2,\mathbb{Z})$.

The center triangle is the Dirichlet region for the group G centered at the point $(0,0)$. Note that this is not a Dirichlet region for $\text{PSL}(2,\mathbb{Z})$, since this group contains an order-three rotation that fixes the center point. $\Diamond$
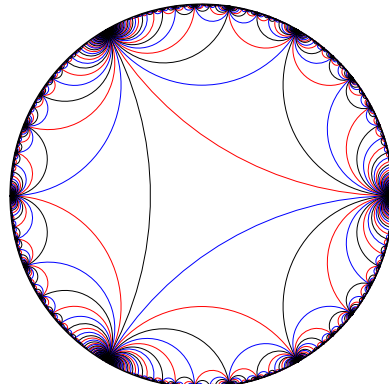
Figure 4.5.1: A tiling of ideal triangles.

4.6 Hyperbolic Surfaces

We have previously talked about surfaces, but with the introduction of hyperbolic geometry, we can now talk about a new type of surface. We first begin by defining a Euclidean surface. The hyperbolic surface will be similar to it.

Definition 4.6.1. A metric surface is *Euclidean* if every point has a neighborhood that is isometric to an open subset of the Euclidean plane. △

Definition 4.6.2. A metric surface is *hyperbolic* if every point has a neighborhood that is isometric to an open subset of the hyperbolic plane. △

We now have two different theorems. We will not prove them here, but instead give resources to find their proof. From [16], we can conclude the following,

Proposition 4.6.3. *Two compact Euclidean surfaces S_1, S_2 are biholomorphic as Riemann surfaces if and only if they are similar. In particular, any biholomorphic map is a Euclidean similarity. Any Euclidean similarity is either biholomorphic or anti-biholomorphic.*

From [15], we have the following.

Proposition 4.6.4. *Two compact hyperbolic surfaces S_1, S_2 are biholomorphic as Riemann surfaces if and only if they are isometric. In particular, any biholomorphic map $S_1 \rightarrow S_2$ is a hyperbolic isometry. Any hyperbolic isometry is either biholomorphic or anti-biholomorphic.*

For a Euclidean surface, the set of all hyperbolic isometries is set of all biholomorphic similarities together with the set of all anti-biholomorphic maps. The biholomorphic maps are orientation-preserving, anti-biholomophic is orientation-reversing.

For a hyperbolic surface, the set of all hyperbolic isometries is set of all biholomorphic isometries together with the set of all anti-biholomorphic maps. The biholomorphic maps are orientation-preserving, anti-biholomophic is orientation-reversing.

Recall the Uniformization Theorem 2.6.9, which tells us that there are can only three isomorphism types of simply connected Riemann surfaces. We will now follow that up with a classification of closed Riemann surfaces.

Theorem 4.6.5 (Classification of Closed Riemann Surfaces). *Any closed Riemann surface is biholomorphic to exactly one of the following:*

- *The Riemann sphere $\widehat{\mathbb{C}}$*

- *A quotient $\mathbb{C}/\Lambda$ where Λ is a lattice $\lambda_1\mathbb{Z} \oplus \lambda_2\mathbb{Z}$.*

- *A quotient $\mathbb{H}/K$ where $K \subset \mathrm{Isom}_+(\mathbb{H})$ acts freely and properly discontinuously.*

Corollary 4.6.6. *If a compact Riemann surface is not biholomorphic to the Riemann sphere or the complex torus, then the complex structure is hyperbolic.*

5
Geometry of Adinkra Embeddings

Let us summarize what we have gotten so far. We want to talk about the geometry of both the adinkras and then surfaces that adinkras embed on. In order to do that, we realized a few things. First, we can embed any graph onto a surface, but we can also treat adinkras as dessins d'enfants, and so they embed onto Riemann surfaces, so the surfaces gain a complex structure. The complex structure of Riemann surfaces with genus greater than 1 have hyperbolic structure, so we needed to study hyperbolic geometry. This actually allows us to talk about the geometry of the surfaces themselves. Furthermore, we would like the adinkra to have nice properties, such as the edges being geodesics on the embedded surface, and the angles between pairs of edges are all equal. We will show that these properties are true for adinkras of $N \geq 4$. Then we apply them to adinkras up to degree 5, which allows us to provide measurements for these adinkra embeddings.

The reason why we need to prove these statements is illustrated to the following example. In figure 5.0.1, we have a graph embedded into a two-holed torus. The two-holed torus has a hyperbolic structure. There are two octagons and two quadrilaterals attached to every vertex. If we assume that the edges are geodesics and the angles between pairs of
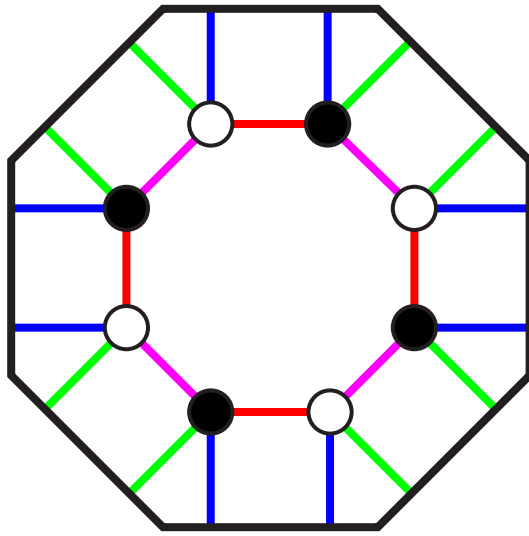
Figure 5.0.1: An embedding of $K_{4,4}$ into a two-holed torus, where the opposite edges of the octagon are identified.

edges are equal, we can conclude that the quadrilateral faces have all right angles, which is something that cannot exist in the hyperbolic plane.

This counterexample illustrates that we will need to do some work to show that a geometric embedding of a graph has nice properties.

5.1 Symmetry of Adinkras through Codes

In this section, we shall show that all adinkra embeddings have the structure that we want, i.e., all angles between adjacent pairs of edges are equal, and all edges are geodesic segments of equal length. We shall do this through codes. We first begin with adinkras equivalent to $\mathbb{Z}_2^N$, using symmetry of this vector space to show that the properties are indeed true for these adinkras. Then we generalize it to all adinkras.

Let I_N be the N-cube adinkra, and let X_N be the surface that I_N embeds on.

Proposition 5.1.1. *There exists a self-equivalence of the dessin (X_N, I_N) that maps the vertex corresponding to the zero vector to any other vertex v_0.*

Proof. Let $h\colon I_N \to I_N$ be a graph automorphism where each vertex $v \in V(I_N)$ goes to $v + v_0$. We note that the vertices $v, v + e_i$ are sent to $v + v_0, v + v_0 + e_i$, so the edges are preserved. Any ribbon structure on the graph is preserved, so the faces are preserved as well. Therefore, h extends to a homeomorphism of X_N to X_N. This allows us to conclude that h induces a self-equivalence of (X_N, I_N). $\square$

Proposition 5.1.2. *There exists a self-equivalence of (X_N, I_N) that fixes v and maps $v + e_i$ to $v + e_{i+1}$ for all i (mod N).*

Proof. By proposition 5.1.1, we can assume that $v = 0$. Let the vertices that are attached to 0 by an edge be denoted by $e_1, e_2, \ldots, e_N$. Let $r\colon I_N \to I_N$ be a graph automorphism that acts on the vertices by cyclicly permuting their coordinates, where the ith coordinate goes to the $i + 1$th coordinate (mod N). Note that r fixes 0, and r maps e_i to e_{i+1} for all i (mod N). Then at every vertex, the attached edges are cyclicly permuted, which preserves both the edges and any given ribbon structure on the graph. Therefore, r extends to a homeomorphism of X_N to X_N. Thus, r induces a self-equivalence of (X_N, I_N). $\square$

Proposition 5.1.3. *There exists a self-anti-equivalence of the dessin (X_N, I_N) that fixes v and $v + e_1$.*

Proof. By propositions 5.1.1 and 5.1.2, we can let $v = 0$. Let the vertices that are attached to 0 by an edge be denoted by $e_1, e_2, \ldots, e_N$. Let X_N^* be the surface obtained from X_N by reversing the orientation. Let $s\colon I_N \to I_N$ be a graph automorphism that acts on the vertices by switching the second coordinate and last coordinate, third coordinate and second-last coordinate, etc. Note that this fixes 0 and e_1. This also switches the vertices e_2 with e_N, e_3 with e_{N-1}, $\ldots$. This preserves the edges, but we can see that the ribbon structure is changed. At every vertex, the cyclic permutation of attached edges is now reversed, so the faces are in the opposite orientation. Therefore, s extends to a

homeomorphism X_N to X_N^*. This means that (X_N, I_N) is equivalent to (X_N^*, I_N), which means that s induces a self-anti-equivalence of (X_N, I_N). $\qquad\square$

Theorem 5.1.4. *For any adinkra isomorphic to $\mathbb{Z}_2^N$, the edges meet at an angle of $2\pi/N$ at each vertex after embedding. If $N \geq 4$, then edges are geodesics segments, and the segments have the same length.*

Proof. By proposition 5.1.2, there exists a self-equivalence of I_N such that for a vertex v of I_N, the vertices $v + e_i$ is mapped to $v + e_{i+1}$ for all $i \pmod{N}$. The self-equivalence induces a biholomorphic map of X_N to itself. This map is conformal, so we can conclude that the angles between pairs of edges must be equal.

By proposition 5.1.3, there exists a self-anti-equivalence of I_N such that v and $v + e_1$ are fixed. This self-anti-equivalence is a anti-biholomorphic map. Since $N \geq 4$, X_N is either a Euclidean or hyperbolic manifold, which means this anti-biholomorphic map is a Euclidean similarity or hyperbolic isometry. This self-anti-equivalence preserves the graph structure, so it must be that the edge between v and $v + e_1$ is preserved. However, a curve whose endpoints are fixed can only be invariant under an orientation-reversing Euclidean similarity or hyperbolic isometry if the curve is a geodesic segment. Thus, the edge must be a geodesic. $\qquad\square$

We have now shown that specific adinkras have geodesic edges of equal length and angles between pairs of edges are equal after embedding. To prove this statement for all adinkras, we will use the fact that any adinkra is the quotient of these adinkras by doubly-even codes .

Let $\mathcal{C}$ be a doubly-even subcode of I_N. Observe that $\mathcal{C}$ is a vector space, so it is a group under vector addition. We can define the group action of $\mathcal{C}$ on I_N by addition of codewords in $\mathcal{C}$. This action then extends to X_N.

Lemma 5.1.5. *Let X_N be a surface onto which I_N embeds. Let $\mathcal{C} \leq \mathbb{Z}_2^N$ be a doubly-even code. Then $\mathcal{C}$ acts freely and properly discontinuously.*

Proof. It can be easily shown from the definition of properly discontinuous that any group action of a finite group is indeed properly discontinuous. Since $\mathbb{Z}_2^N$ is finite, any subset is also finite, and so $\mathcal{C}$ acts properly discontinuously.

We will now prove that the group action of a doubly-even code on I_N is free. Let $v \in I_N$. Let $c \in \mathcal{C} \setminus \{0\}$. C acts on I_N, this action on I_N extends to an action on X_N. We must show that C has no fixed points on X_N.

First, we observe that no vertex is a fixed point since the group action of a code adds c to v.

We will show that no edge has a fixed point. The vector v is connected to $v + e_1, v + e_2, \ldots, v + e_N$, where e_i is zero in all coordinates except for the ith coordinate where it is 1. First, the edge with endpoints v and $v + e_i$ has a fixed point if the group action switches v and $v + e_i$. But since c is doubly even, this is not possible, as we get that at least 4 coordinates must change from the group action.

We will now show that no face has a fixed point. The face with vertices $v, v + e_i, v + e_j, v + e_i + e_j$ has a fixed point if the group action permutes the vertices. However, since we have that c is doubly-even, the group action will change at least 4 coordinates, and so there is no way for the vertices to permute.

Thus, the action does not fix any vertex, edge, or face, so the action does not fix any point, and we get that the group action is free. $\qquad\square$

Theorem 5.1.6. *Let $A = I_N/\mathcal{C}$ be an adinkra where $\mathcal{C}$ is a doubly-even subcode of $\mathbb{Z}_2^N$. Let X_N be the Riemann surface on which I_N embeds, and let X be the Riemann surface on which A embeds. Then there exists a holomorphic covering map from $X_N \to X$ that restricts to the quotient map $I_N \to A$.*

Proof. By lemma 5.1.5, $\mathcal{C}$ acts freely and proper discontinuously on X_N. Thus, X is homeomorphic $X_N/\mathcal{C}$.

Let $p\colon X_N \to X$ be the associated covering map. We note that p maps I_N to A. a graph embedded on X will lift into X_N. Let X'_N be the surface isomorphic to X_N but with induced complex structure by lifting the complex structure from X. The identity $id\colon X_N \to X'_N$ is an equivalence of dessins that maps I_N in X_N to I_N in X'_N that restricts to id on I_N. By the Grothendieck correspondence 3.3.7, we get a biholomorphic map h from X_N to X'_N that restricts to id on I_N.

Then $p \circ h$ is the desired covering map. $\qquad\square$

Corollary 5.1.7. *For any adinkra $N \geq 4$, the edges are geodesic segments that meet at an angle of $2\pi/N$, and all edges have the same length.*

5.2 Geometry of $N \leq 4$ Adinkras

In each of the subsections, we will talk about the $N = 2, 3, 4$ adinkra embeddings in that order.

5.2.1 $N = 2$ Adinkras

We shall begin with the $N = 2$ adinkra, for it is the most simple adinkra with a meaningful embedding. The $N = 2$ adinkra embeds on a Riemann sphere. We can have that the 4 vertices are located at $0, 1, -1, \infty$ on the Riemann sphere.

We first note that the complex structure does not induce a spherical geometry, so our argument in section 5.1 does not apply. However, we can get around this by finding a Belyi function.

Proposition 5.2.1. *Let $f\colon \widehat{\mathbb{C}} \to \widehat{\mathbb{C}}$ be a function defined by*

$$f(z) = \left(\frac{1 - z^2}{1 + z^2}\right)^2.$$

Then f is a Belyi function.

Proof. It can be easily shown that this function maps $1, -1$ to 0, $0, \infty$ to 1, and $i, -i$ to ∞.

Now we show that for all real numbers in the domain, f maps it to $[0, 1]$. Observe that $f(x)$ is a real number for all $x \in \mathbb{R} \cup \{\infty\}$. Now consider

$$\frac{1 - z^2}{1 + z^2} = \frac{1 + z^2 - 2z^2}{1 + z^2} = 1 - 2\frac{z^2}{1 + z^2}.$$

Let $g(z) = \frac{z^2}{1+z^2}$. It is sufficient to show that $g(\mathbb{R} \cup \{\infty\}) \subseteq [0, 1]$. We note that both z^2 and $1 + z^2$ are always non-negative numbers for any real number, so their quotient must be non-negative. We also note that $z^2 < 1 + z^2$, so this implies that $\frac{z^2}{1+z^2} < 1$. Thus, we can conclude that $f(\mathbb{R} \cup \{\infty\}) \subseteq [0, 1]$. $\qquad\square$

Proposition 5.2.2. *There exists an embedding of the $N = 2$ adinkra onto the sphere where the angles between edges of the $N = 2$ embedding is π, and the length of the edges is $\pi/2$.*

Proof. Since each vertex has two edges attached and the angles between each pair of edges must be equal, we have that the angle must be $2\pi/2$ or just simply π.

The circumference of the great circles on the Riemann sphere is 2π. Since the 4 edges form a great circle, and all edges have the same edge length, it must be that each edge has a length of $\pi/2$. $\qquad\square$

The final note is that this adinkra embedding is unique up to scaling. We chose the Riemann sphere, but in reality, this can embed on any sphere of any radius. The angle will stay the same, but the edge length will scale up accordingly.
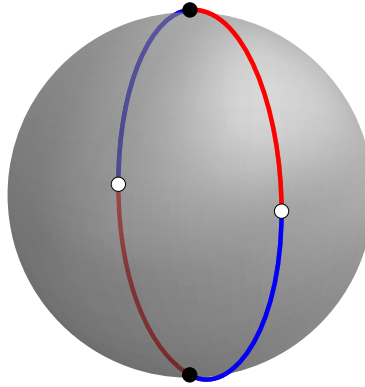
Figure 5.2.1: The square adinkra embedded in the sphere.

5.2.2 *N = 3 Adinkras*

The $N = 3$ adinkra also embeds on a Riemann sphere. We note again that the complex structure does not induce a spherical geometry. This time, finding a Belyi function is much more difficult. Still, there is a nice embedding of this adinkra on the sphere that maps edges to geodesics segments of equal length with the angles between pairs of edges being $2\pi/N$.

We can easily calculate the angle between the edges to be $2\pi/3$. Since this is on the Riemann sphere, we can use spherical geometry to figure out the edge lengths. A resource is available in [20].

Proposition 5.2.3. *There exists an embedding of the $N = 3$ adinkra onto the sphere where the edge length is*

$$\cos^{-1}\frac{1}{3} \approx 1.23096.$$

Proof. From [20], we get *dual spherical law of cosines*

$$\cos C = -\cos A \cos B + \sin A \sin B \cos c,$$

where A, B, C are angles of a triangle, and c is the length of the side opposite C. We use the figure 5.2.2 to fill in the proper angles. Let a be the length of the side opposite the

angle $\pi/3$. In order to find a, observe that

$$\cos\frac{\pi}{3} = -\cos\frac{\pi}{3}\cos\frac{2\pi}{3} + \sin\frac{\pi}{3}\sin\frac{2\pi}{3}\cos a$$
$$= \frac{1}{4} + \frac{3}{4}\cos a.$$

This implies that $\cos a = \frac{1}{3}$, and thus the edge length is $\cos^{-1}\frac{1}{3}$. $\qquad\square$
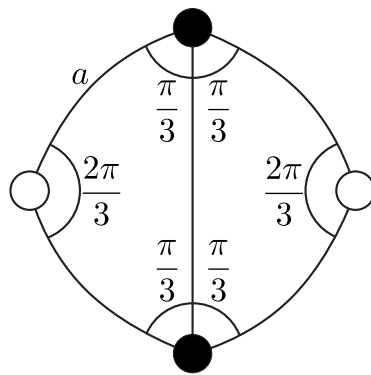
Figure 5.2.2: A square face of the cube adinkra embedded, with a diagonal used to create a triangle used to find the edge length.
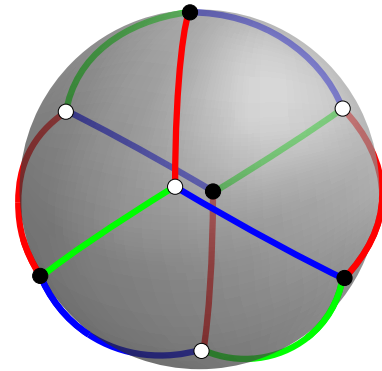
Figure 5.2.3: The cube adinkra embedded on the sphere.

5.2.3 $N = 4$ *Adinkras*

There exists two $N = 4$ adinkras. Both adinkras embed on a complex torus after calculation of their genus by proposition 3.4.4. We will claim that these two adinkras embed on the complex torus $\mathbb{C}/(\ell\mathbb{Z} \oplus i\ell\mathbb{Z})$ for $\ell > 0$, i.e., this embeds on the square torus with side length ℓ. We will first talk about the $n = 3, N = 4$ adinkra.

This is the first adinkra that we can apply section 5.1. In figure 5.2.4, note that if we have a graph automorphism by rotating counterclockwise around any black vertex, we end up cyclicly permuting the edge colors by (Red, Pink, Green, Blue). Any graph automorphism by rotating counterclockwise around any white vertex ends up permuting the edge colors by (Red, Blue, Green, Pink). Either permutation does not change the rainbow. Therefore,

rotations are also homeomorphisms of the surface, so the angles between adjacent pairs of edges must be equal. We also note that since rotations are graph automorphisms, the edges are preserved, and so all edges must be the same length.

Now suppose that we have a graph automorphism that reflects across a line determined by a white vertex v_1 and an adjacent black vertex v_2. The reflection will change the rainbow by (Red, Green), so the rainbow is reversed. Thus, reflections reverse the orientation of the surface of which the graph is embedded on. Since the vertices v_1, v_2 are preserved, the edge between them must also be preserved and therefore it must be a geodesic segment.

Since this adinkra embeds on a torus, then we will just look at the square with opposite edges identified with side length ℓ. Since the complex structure is Euclidean, it is similar(or homothetic), so the exact side length does not matter.

Proposition 5.2.4. *For the $n = 3, N = 4$ adinkra embedding into the square torus, the angles between each edge is $\pi/2$. The edge lengths are $\ell\sqrt{2}/4$.*

Proof. At each vertex, there are 4 edges, so the angle between each pair of edges is $2\pi/4$ or just $\pi/2$.

The fundamental region is a square of side length ℓ. The length of the diagonal of the fundamental region is $\ell\sqrt{2}$. There are 4 edges on the diagonal, so the edge length is $\ell\sqrt{2}/4$. $\qquad\qquad\square$

We will now look at the $n = 4, N = 4$ adinkra. This adinkra also embeds onto a torus, so we again look at the square with side length ℓ in the Euclidean plane.

We first note that since the number of edges is still 4 per vertex, the angle between adjacent pairs of edges does not change and is $\pi/2$.

Proposition 5.2.5. *For the $n = 4, N = 4$ adinkra embedding into the square torus, the edge lengths are $\ell/4$.*
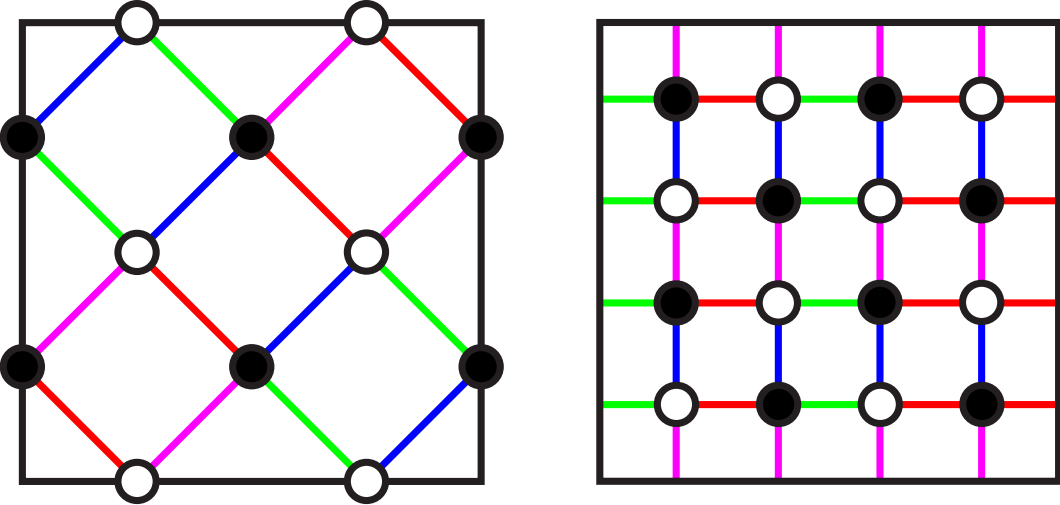
Figure 5.2.4: The left is the $n = 3, N = 4$ adinkra embedded onto a torus. The right is the $n = 4, N = 4$ adinkra embedded onto a torus.

Proof. Note that the edges are parallel to the boundary, as seen in figure 5.2.4. Since there are 4 edges per line, we have that each edge is 1/4 of the total length. The length of the boundary is ℓ, so the edge length is $\ell/4$. □

5.3   Geometry of $N = 5, n = 4$ Adinkra

The really interesting case is the situation when $N = 5$. There are actually two $N = 5$ adinkras, one with 16 vertices and one with 32. We will study the one that has 16 vertices. This adinkra that we will study is also isomorphic to $\mathbb{Z}_2^5/\{00000, 11110\}$. First of all, after calculation of the Euler characteristic by proposition 3.4.4, we get that this adinkra embeds onto the 3-holed torus. Thus by theorem 4.6.5, the complex structure of the surface is hyperbolic.

We note another thing about the choice of rainbow. There is in fact an edge color that has a special property. This special property is that if we remove all edges of this specific color, the adinkra topology becomes disconnected. Even though there is a special edge color, there still is only one choice of rainbow, in that our choice of rainbow does not affect the embedding. This is because with only one special edge color, we are able to permute the other 4 colors and still end up with any cyclic permutation.

To be clear, we will now mention our edge colors is the set $\{e_1, e_2, e_3, e_4, e_5\}$, and the rainbow will be the same order as listed. That means that for white vertices, the rainbow will be the counterclockwise order, and for black vertices, the rainbow will be the clockwise order. In our diagrams, we have that Red represents e_1, Blue represents e_2, Green represents e_3, Brown represents e_4, and Purple represents e_5.

The special edge is e_5. This edge color connects even codewords and odd codewords. Thus, there are two sets of codewords, the even codewords and odd codewords. Note that this is not the same bipartition of vertices into black vertices and white vertices.

We will now attempt to find fundamental regions for our adinkra embedding. This is where we explain the algorithm of finding the following results. We have an adinkra embedded in a hyperbolic surface. The universal cover of this surface is the hyperbolic plane. We know that the face measurements of the embedding are determined, so there is
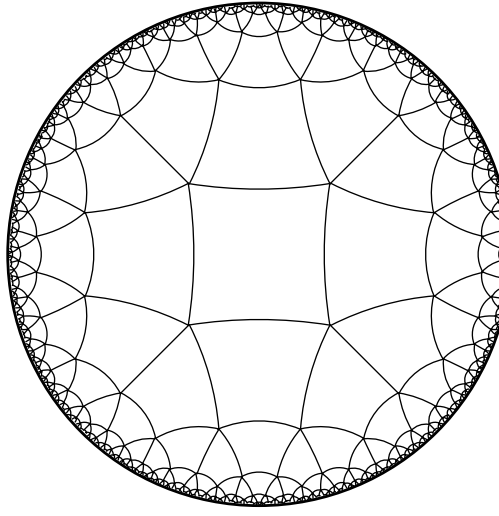
Figure 5.3.1: The initial setup of tiling the plane with squares such that there are 5 squares that meet at every vertex.
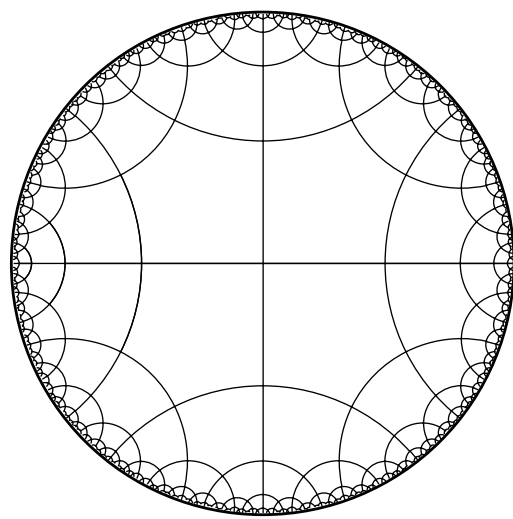
Figure 5.3.2: Finding the dual tesselation to the square tiling.

only one way to tiling the hyperbolic plane with squares such that 5 squares meet at every vertex, as shown in figure 5.3.1. In reality, this tiling can be hard to work with, so we will construct the *dual* to this tiling, which is a tiling of pentagons such that 4 pentagons meet at every vertex. This is shown in figure 5.3.2. Now we explain the algorithm.

Algorithm 5.3.1.

1. Mark the center point, and find other locations of this point in the tiling.

2. Find the perpendicular bisectors of the other points with the center point, and this will create a Dirichlet region.

Figure 5.3.3 shows this algorithm being applied. ◇

We now will talk about figuring out lengths of the pentagonal tiling. While we do not know directly how to calculate anything related to pentagons, we can do something clever. We can draw line segments from the center point of each pentagon to each of its five
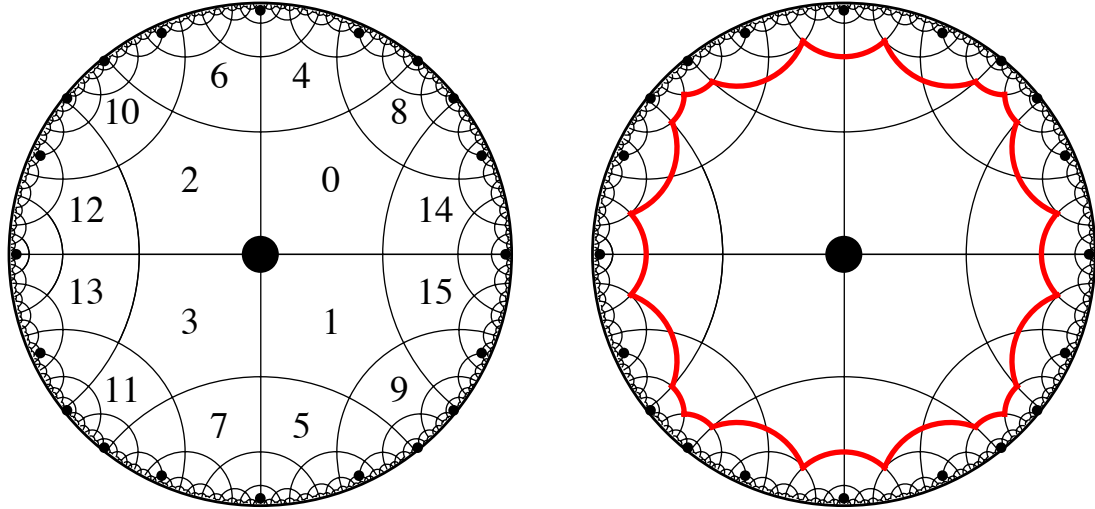
Figure 5.3.3: An illustration of the algorithm to find Dirichlet regions.

vertices, as well as to the midpoint of each side, forming a triangulation of the hyperbolic plane, as shown in figure 5.3.4. The lengths of these line segments have special names.
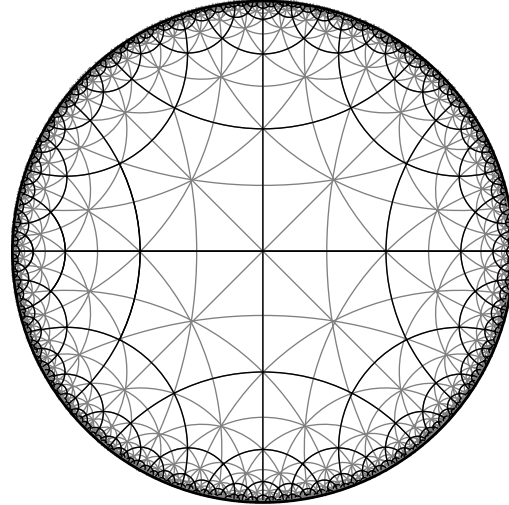
Figure 5.3.4: Tiling of triangles after the apothem and circumradii of the pentagons have been drawn.

Definition 5.3.2. The *apothem* of a regular polygon is the length from the center to the midpoint of one of its edges. The *circumradius* of a polygon is the length of the radius of its circumscribed circle. Alternatively, for a regular polygon, the circumradius is the

length from the center to one of its vertices. The *height* of a regular polygon with an odd number of sides is the sum of its apothem and its circumradius. △

Now that we have a triangulation, we can use the formulas in section 4.4 to calculate the side lengths of these triangles. As it will turn out, these lengths are essential to figuring both the side lengths and angles that we are interested in and will be used very often.

Proposition 5.3.3. *Let s be the side length of the pentagon. Let a be the apothem. Let c be the circumradius. The side length, apothem, and circumradius of the pentagon with five right angles in the hyperbolic plane are*

$$
s = \cosh^{-1}\left(\frac{1 + \sqrt{5}}{2}\right), \qquad a = \cosh^{-1}\sqrt{1 + \frac{1}{\sqrt{5}}}, \qquad c = \cosh^{-1}\sqrt{1 + \frac{2}{\sqrt{5}}},
$$

respectively.

Proof. We will first figure out the side length of the pentagon. Consider the triangle with one side being side of the pentagon and the other two sides being the circumradius of the pentagon. Let this triangle be $\mathcal{T}_1$. Since we know that there are 5 circumradii evenly dividing the center point, we have that one of the angles in the triangle is $2\pi/5$. The other two angles are $\pi/4$. Now that we know all three angles of $\mathcal{T}_1$, we can use the dual hyperbolic law of cosines to figure out all three side lengths of the triangle. Observe that

$$
\cos\frac{2\pi}{5} = -\cos\frac{\pi}{4}\cos\frac{\pi}{4} + \sin\frac{\pi}{4}\sin\frac{\pi}{4}\cosh s,
$$

and

$$
\cos\frac{\pi}{4} = -\cos\frac{2\pi}{5}\cos\frac{\pi}{4} + \sin\frac{2\pi}{5}\sin\frac{\pi}{4}\cosh a.
$$

The results for s and a follow from these calculations.

In order to find c, we form the triangle $\mathcal{T}_2$ where the three sides are the apothem, the circumradius, and half of the edge of the pentagon. Since the circumradius intersects the pentagon edge at a right angle, this triangle is a right angle, so we can use the hyperbolic

Pythagorean theorem. Observe that

$$\cosh a = \cosh \frac{s}{2} \cosh c.$$

The result for c follows from this calculation. □

Proposition 5.3.4. *Let h be the height of the pentagon. The height of the pentagon with five right angles in the hyperbolic plane is*

$$h = \sinh^{-1} \sqrt{2 + \sqrt{5}}.$$

Proof. Since we have both the apothem and the circumradius, we can calculate their sum to get the height. We use Mathematica to simplify this expression to get that $\cosh^{-1} \sqrt{1 + \frac{1}{\sqrt{5}}} + \cosh^{-1} \sqrt{1 + \frac{2}{\sqrt{5}}} = \sinh^{-1} \sqrt{2 + \sqrt{5}}$. As a result, we get that

$$h = \sinh^{-1} \sqrt{2 + \sqrt{5}}.$$

□
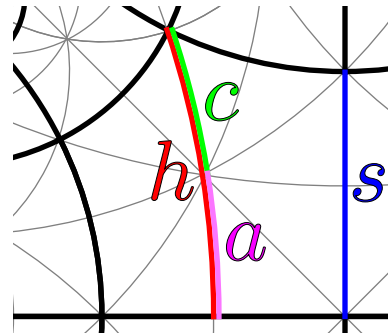
Figure 5.3.5: The blue edge is the side length, the red edge is the height of the pentagon, the pink edge is the apothem, and the green edge is the circumradius.

We end this section by figuring out the geometry of the $N = 5$ adinkra.

Proposition 5.3.5. *The angle is $2\pi/5$. The edge length is $\cosh^{-1}(1 + \frac{2}{\sqrt{5}})$.*

Proof. At each vertex, there are 5 edges, so the angle between each pair edges is $2\pi/5$.
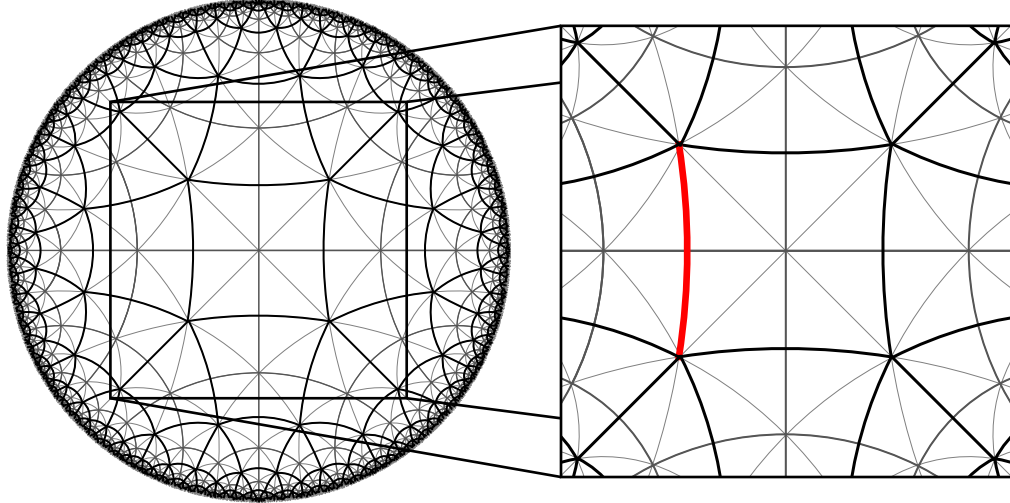
Figure 5.3.6: Note that the edge of a square, marked in red, is twice the apothem of the pentagon.

From figure 5.3.6, we can observe that the edge length is twice the apothem, so we conclude that it is $2a = 2\cosh^{-1}\sqrt{1 + \frac{1}{\sqrt{5}}}$. We apply proposition 4.4.6 to get that the edge length is $\cosh^{-1}(1 + \frac{2}{\sqrt{5}})$. $\square$

5.3.1   *16-Sided Polygonal Dirichlet Region*

Our goal now is to find a Dirichlet region with the symmetry group of D_4. From algorithm 5.3.1, we take the point in the center, which is determined by the four surrounding pentagons, find its orbit, and find a Dirichlet region from the orbit of the this point. Figure 5.3.7 shows the number tiling of this. With these results, our Dirichlet region is a 16-sided polygon, or a *hexadecagon*. We will now try to figure out the geometry of this Dirichlet region, meaning the side lengths of this polygon, as well as the interior angles.
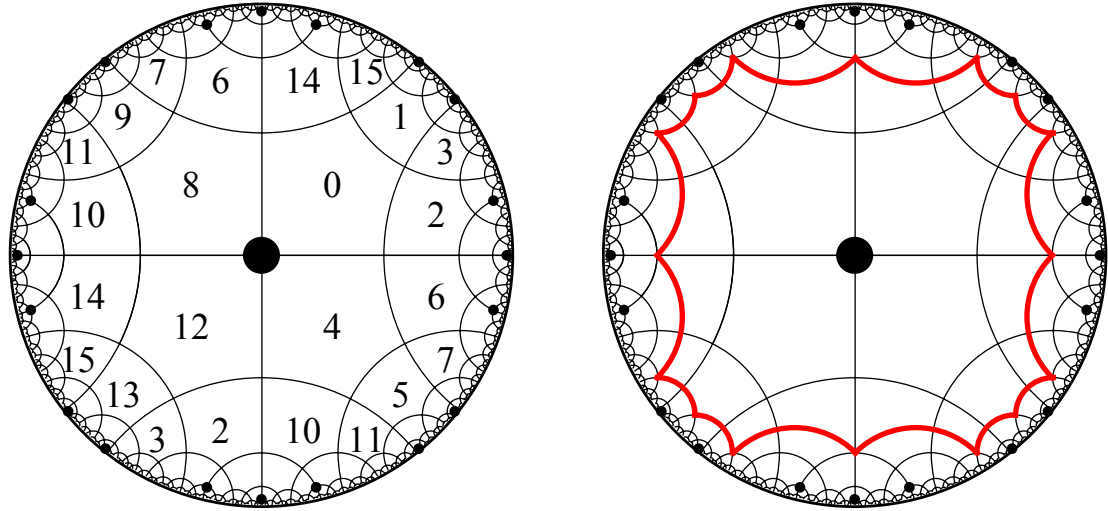
Figure 5.3.7: The left has the tiling used to find the dirichlet region of 16 sides, with black dots to mark the orbit of the center point. The right shows the dirichlet region marked in red.
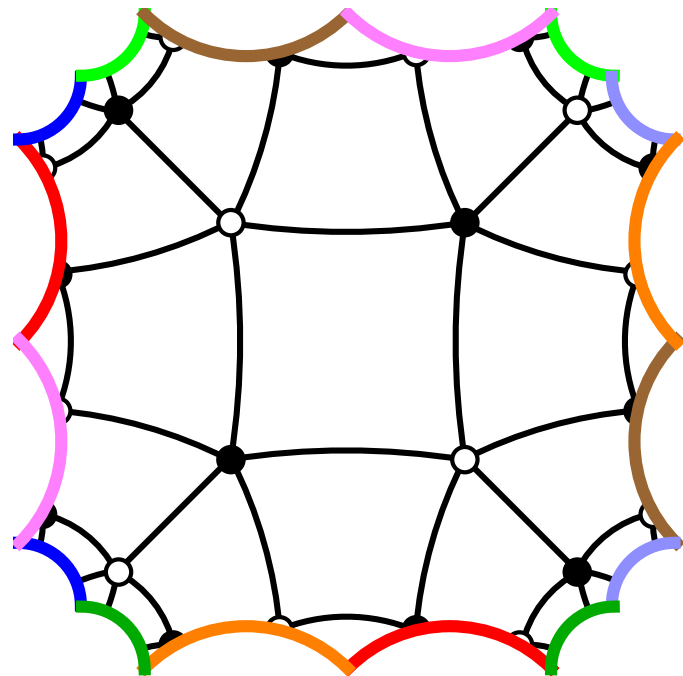
Figure 5.3.8: Hexadecagon Dirichlet Region where same color edges are identified and adinkra topology embedded.
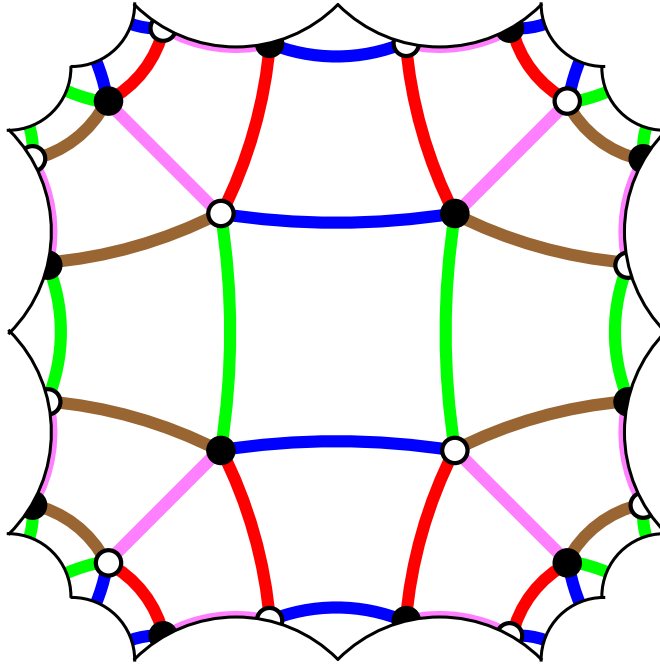
Figure 5.3.9: Hexadecagon Dirichlet Region with adinkra chromotopology.

Proposition 5.3.6. *The Dirichlet region of 16 sides has 2 different edge lengths, P, R, as seen in figure 5.3.10. They are*

$$P = \cosh^{-1}(5 + 2\sqrt{5}) \approx 2.9387$$

$$R = \cosh^{-1}(2 + \sqrt{5}) \approx 2.12255.$$

Proof. From figure 5.3.11, we note that P is twice the height of the pentagon, resulting in $2\sinh^{-1}\sqrt{2 + \sqrt{5}}$. We apply proposition 4.4.6 to get that this is equal to $\cosh^{-1}(5 + 2\sqrt{5})$. From figure 5.3.12, we note that R is twice the side length of one of the pentagons, so we get $2\cosh^{-1}\left(\frac{1+\sqrt{5}}{2}\right)$. We apply proposition 4.4.6 to get the result of $\cosh^{-1}(2 + \sqrt{5})$. $\square$

Proposition 5.3.7. *The Dirichlet region of 16 sides has 2 angles as seen in figure 5.3.10. They are $\pi/2$ and $\pi/4$.*

Proof. From figure 5.3.10, we note that there are three different angles: the angle between two edges of length P, the angle between an edge of length P and an edge of length R,
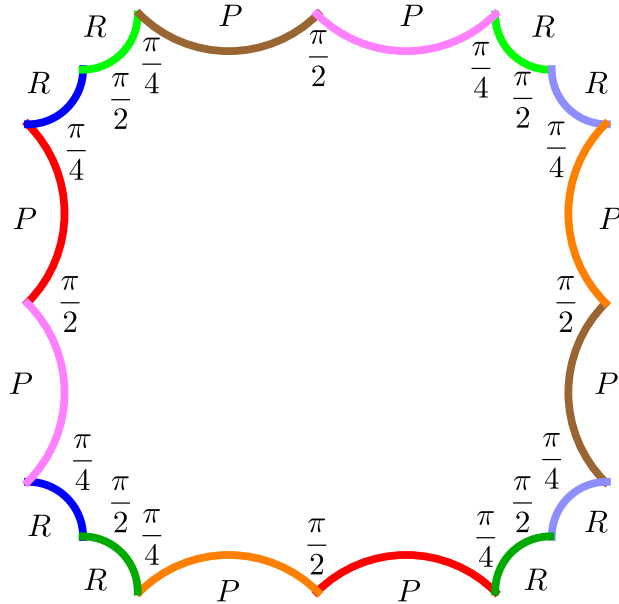
Figure 5.3.10: Hexadecagon Dirichlet Region with the two side lengths and the two angles labeled.

and the angle between two edges of length R. When two edges of length P and P meet, we can see from figure 5.3.13 that each edge is an angle bisector to a pentagon. Thus, we get that the angle is $\pi/2$. From figure 5.3.14, when an edge of length P and an edge of length R meet, the edge of length P is still an angle bisector, while the edge of length R is an edge of a pentagon. Thus, the angle is $\pi/4$. Also in the same figure 5.3.14, when two edges of length R meet, both edges are edges of the same pentagon, so the angle is $\pi/2$. $\qquad\square$

Now we note the symmetry group of this Dirichlet region.

Proposition 5.3.8. *The Dirichlet region has D_4 symmetry, where D_4 is the dihedral group of the square.*

Proof. Horizontal reflections switch:

- Red with Orange,

- Blue with Light Blue,

- Brown with Pink.

Vertical reflections switch:

- Red with Pink,

- Green with Dark Green,

- Brown with Orange.

Rotation by $\pi/2$ switches:

- Red $\to$ Orange $\to$ Brown $\to$ Pink $\to$ Red,

- Blue $\to$ Dark Green $\to$ Light Blue $\to$ Green $\to$ Blue.

For the adinkra, reflections both horizontally and vertically preserve all edge colors in the adinkra.

For rotation by $\pi/2$, we first note that black vertices and white vertices switch. We also note that blue edges switch with green edges and red edges switch with brown edges. Edges colored pink, our special edge color, are not affected. This rotation actually reverses the cyclic ordering of our rainbow, but since black and white vertices are also switched, this means that the rainbow is entirely preserved.

Thus, we get the D_4 symmetry group. $\square$
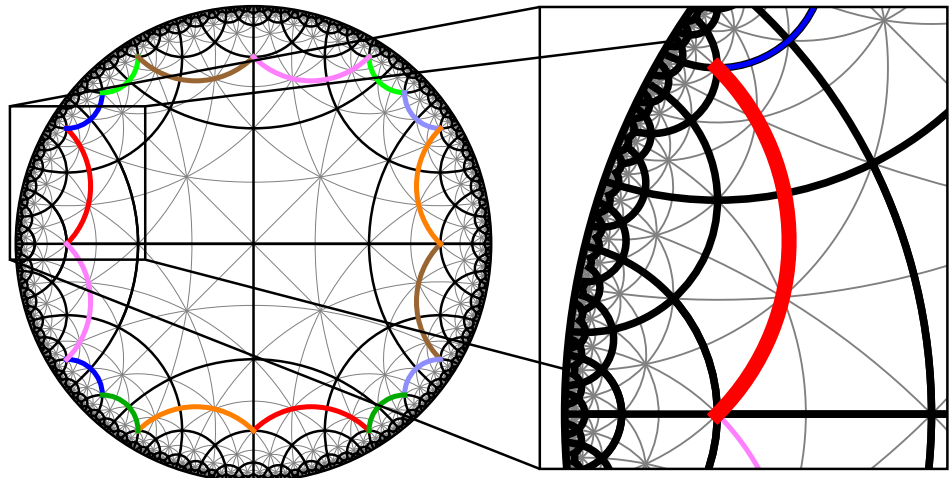
Figure 5.3.11: Observe that the red edge is twice the height of a pentagon.
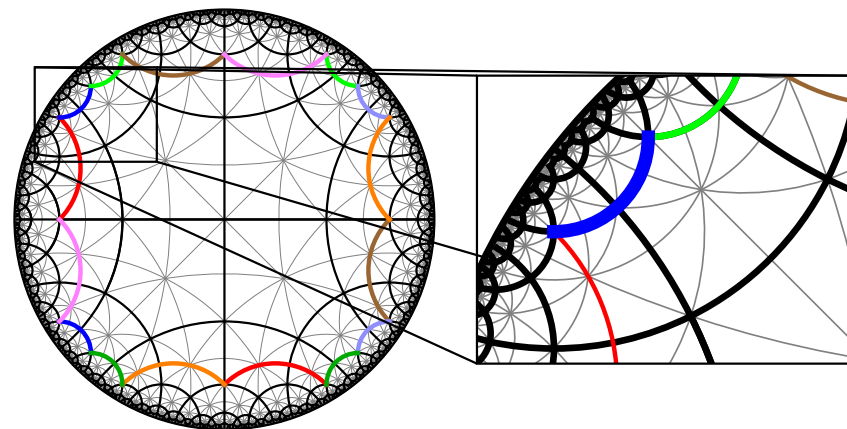

Figure 5.3.12: Observe that the blue edge is twice the side length of a pentagon.
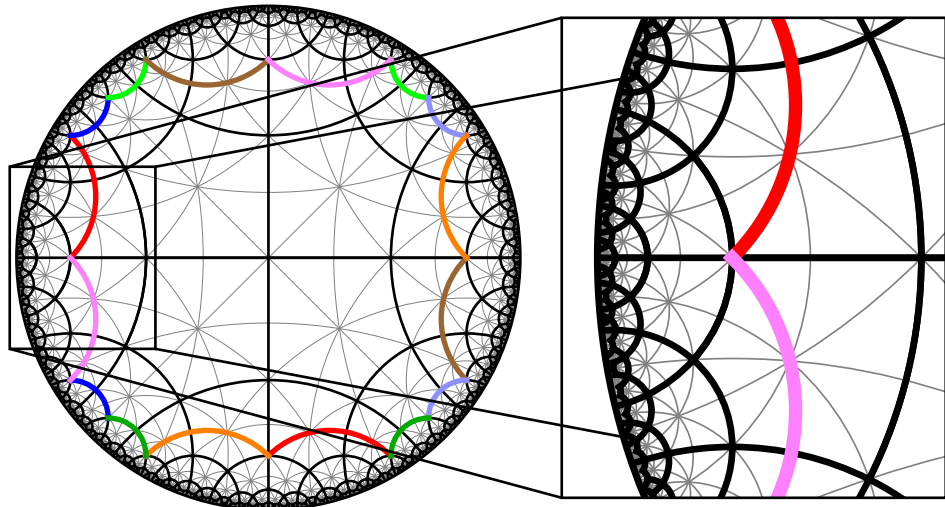
Figure 5.3.13: The first angle bisects two right angles, so the angle is a total of $\pi/2$.
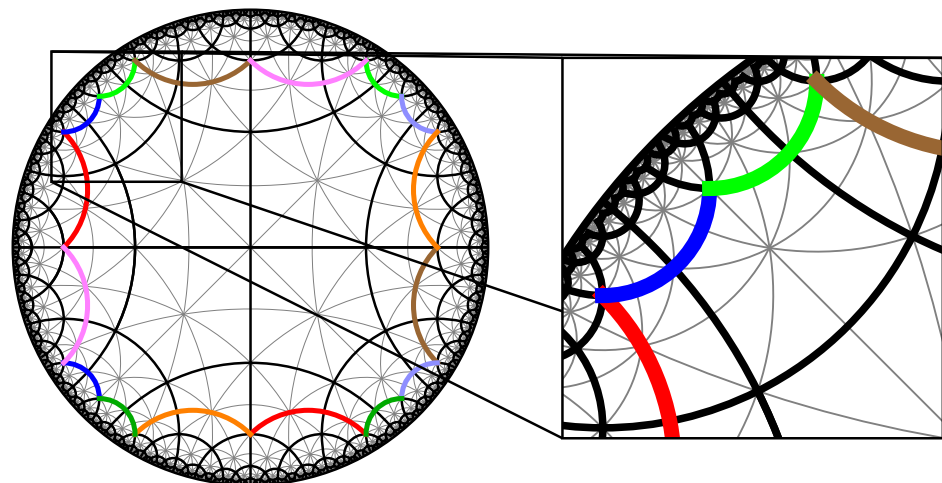

Figure 5.3.14: The second half bisects one right angle, so the angle is $\pi/4$.
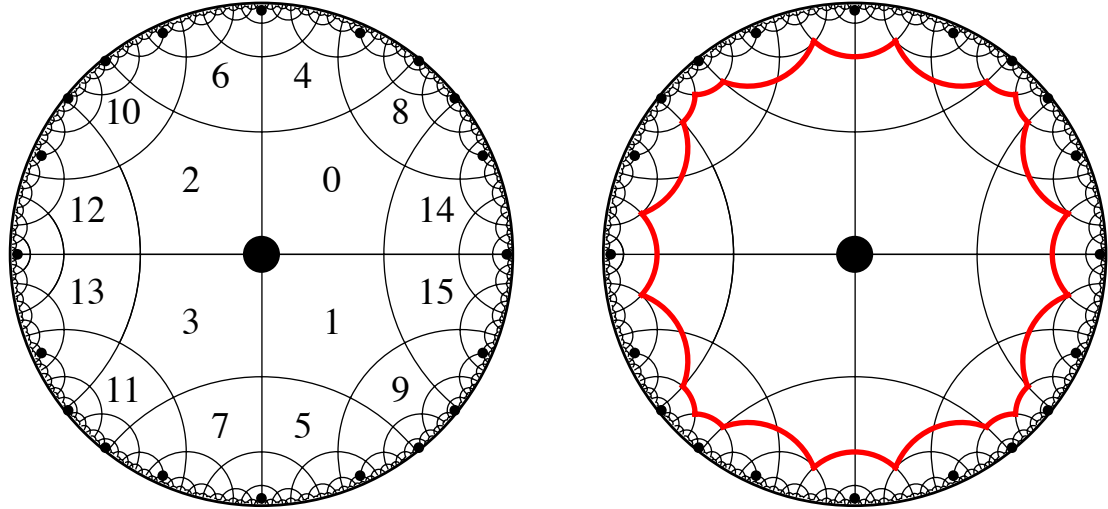
Figure 5.3.15: The tiling used to find the dirichlet region of 20 sides.

5.3.2 Dodecagon Fundamental Region

We initially began finding a Dirichlet region which ended up being a 16-sided polygon. This 16-sided polygon is also a fundamental domain for our surface which the adinkra is embedded on. For a 3-holed torus, the fundamental domain with the least number of sides is 12, meaning it can be a dodecagon. We will now try to find it.

Using the algorithm 5.3.1, we will now attempt to find a different Dirichlet region. The pentagons that will surround the center point will be $0, 1, 2, 3$, and we will take the orbit of this point. The Dirichlet region we ended up getting is a 20-sided polygon, as shown in figure 5.3.15. Using some cutting and splicing, we can manipulate this 20-sided polygon into a dodecagon, as seen in figure 5.3.16 and figure 5.3.16.

Now that we have found a dodecagon, we will now try to figure out its side lengths and interior angles.
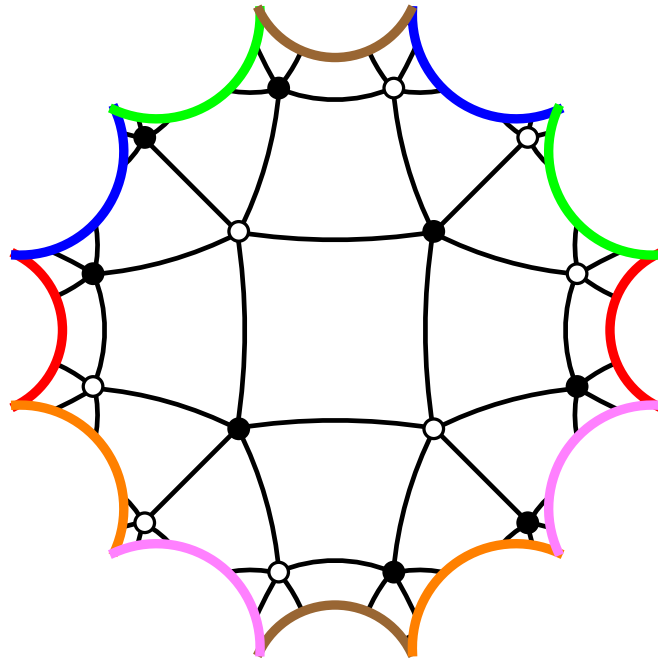
Figure 5.3.16: The Dodecagonal Fundamental Region, with the $N = 5$ adinkra topology. The same color edges of the dodecagon are identified with each other.
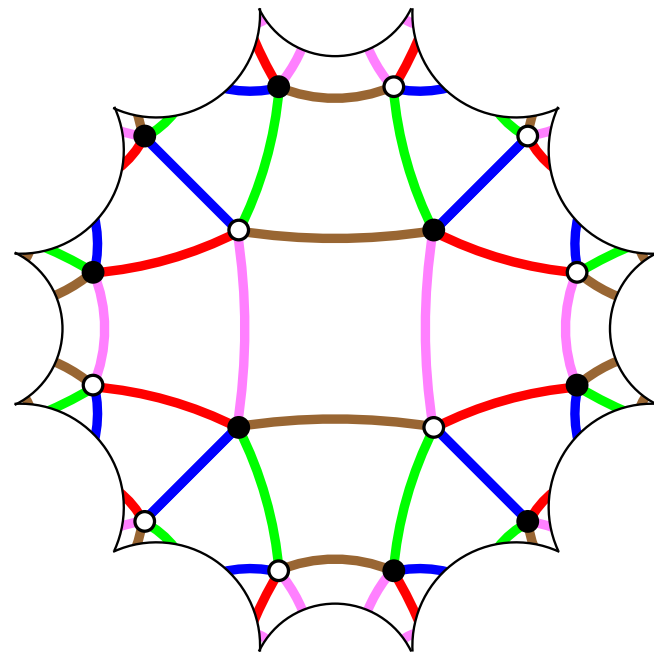

Figure 5.3.17: The Dodecagonal Fundamental Region, with the $N = 5$ adinkra chromo-topology.
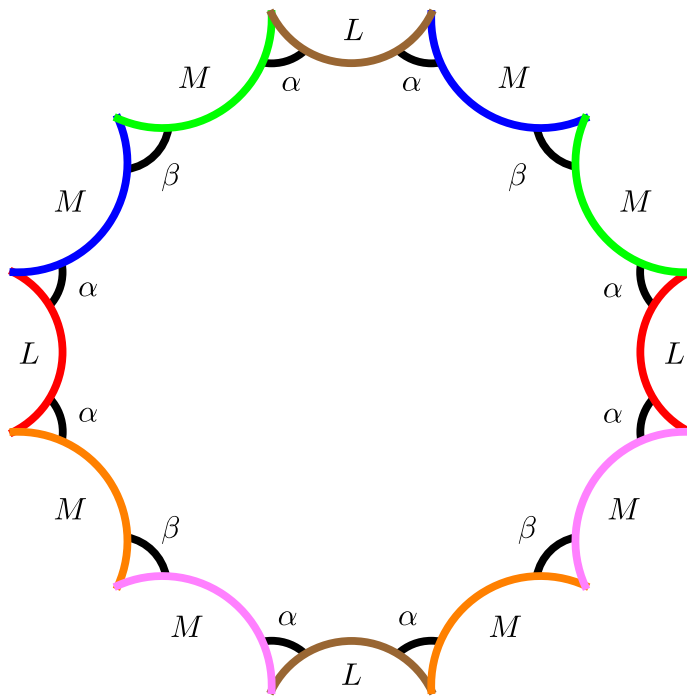
Figure 5.3.18: Dodecagon Fundamental Region with the two side lengths and the two angles labeled.

Proposition 5.3.9. *The dodecagonal fundamental region has 2 different edge lengths, L, M, as seen in figure 5.3.18. The two edge lengths are as follows*

$$L = \cosh^{-1}(17 + 8\sqrt{5}) \approx 4.2451$$

$$M = \cosh^{-1}(13 + 6\sqrt{5}) \approx 3.96677.$$

Proof. We first observe that the shape of the dodecagon has D_4 symmetry. From figure 5.3.18, we observe that the red and brown edges have length L. The blue, green, pink and orange edges have length M.

From figure 5.3.19, we have that L is actually just four times the side length of the pentagon. Thus, L is $4s$. Then we apply proposition 4.4.6 twice to get the result of $\cosh^{-1}(17 + 8\sqrt{5})$.

We now turn our attention to finding out the other side length. From figure 5.3.20, we will argue that point p is in fact the midpoint of an edge of length M. When we rotate around p by π, we get that the pentagons labeled 4 and 12 are switched. The pentagons labeled 8 and 10 are also switched. Thus, the endpoints of the blue edge are switched, which allows us to conclude that p is indeed the midpoint of the blue edge.

So we will just find out half of the length of M, and then multiply it by 2.

Let b be half the length of M. From figure 5.3.21, we formed a triangle with edge lengths $2s, h, b$, and the angle opposite to b is $\frac{\pi}{4}$. Thus, we use the hyperbolic law of cosines to get that

$$\cosh b = \cosh(2s) \cosh h - \sinh(2s) \sinh h \cos \frac{\pi}{4}.$$

We can simplify the right-hand side to get that $\cosh b = \sqrt{7 + 3\sqrt{5}}$, and M is $2b$. We apply proposition 4.4.6 to get that $2b = \cosh^{-1}(13 + 6\sqrt{5})$. $\qquad\square$

Proposition 5.3.10. *The dodecagonal fundamental region has 2 angles α, β as shown in figure 5.3.18. They are*

$$\alpha = \cos^{-1} \sqrt{\frac{5}{6}} \approx 24.0948°$$

$$\beta = \cos^{-1} \frac{\sqrt{5}}{3} \approx 41.8103°.$$

Proof. We note that α is the angle between L and M, and β is the angle between M and M.

We look at figure 5.3.21, and observe the triangle with angle $\pi/4$ and sides $2s, h$, and b. Note that α is the angle opposite side h. We want to find this angle, so we use the law of cosines to get

$$\cosh h = \cosh(2s) \cosh b - \sinh(2s) \sinh b \cos \alpha.$$

We are able to simplify this expression and get that $\cos \alpha = \sqrt{\frac{5}{6}}$.

For β, we observe from figure 5.3.22, we have an isosceles triangle with sides $b, b, 2s$. The angle opposite $2s$ is β, so we will use the hyperbolic law of cosines to get

$$\cosh(2s) = \cosh b \cosh b - \sinh b \sinh b \cos \beta.$$

When we simplify this expression, we get that $\cos \beta = \frac{\sqrt{5}}{3}$. $\qquad \square$

The final observation of this dodecagon is its symmetry group.

Proposition 5.3.11. *The symmetry group of this dodecagon in the hyperbolic plane is the Klein-4 group.*

Proof. First, we note that the dodecagon shape itself has D_4 symmetry, so automorphisms of the shape include reflections both horizontally and vertically, as well as rotations by $\pi/2$.

In figure 5.3.16, there are a total of six pairs of edges. We consider how pairs of edges of the dodecagon are identified and see which of the group actions of D_4 preserves them.

When we reflect horizontally, we switch the blue edges with the green edges, as well as switch orange edges with pink edges. Thus, horizontal reflection is an automorphism.

When we reflect vertically, we switch blue edges with orange edges and switch green edges with pink edges. So we have that vertical reflection is also an automorphism.

When we reflect this region, we can also consider how the adinkra changes. In both reflections horizontally and vertically, the same edge colors goes to the same edge colors.

Now we consider counterclockwise rotation by $\pi/2$. This is not an automorphism. For example, when we consider the green and orange edges, we have that one green edge goes to another green edge, but the other green edge goes to orange.

When we consider how rotation affects the adinkra, we have that pink edges of the adinkra switches with brown edges of the adinkra. We also have that red edges switch with green edges. This is bad as it does not preserve the rainbow.

Since horizontal and vertical reflections are automorphisms, but rotation is not an automorphism, we conclude that the symmetry group is indeed the Klein-4 group. $\qquad\square$

While we have figured out the fundamental domain of the least number of sides, there are some sacrifices. The measurements do not compare so nicely to the Dirichlet region of 16 sides, and the symmetry group is smaller, meaning it has less symmetry.
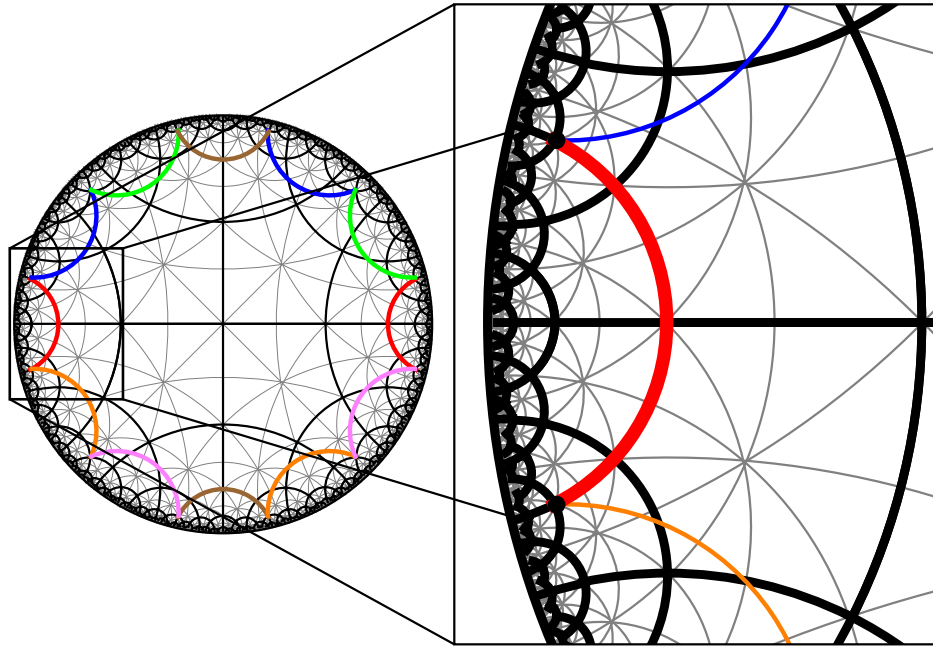
Figure 5.3.19: Observe that the red edge separates the 4 pentagons on the left with the 4 pentagons on the right.
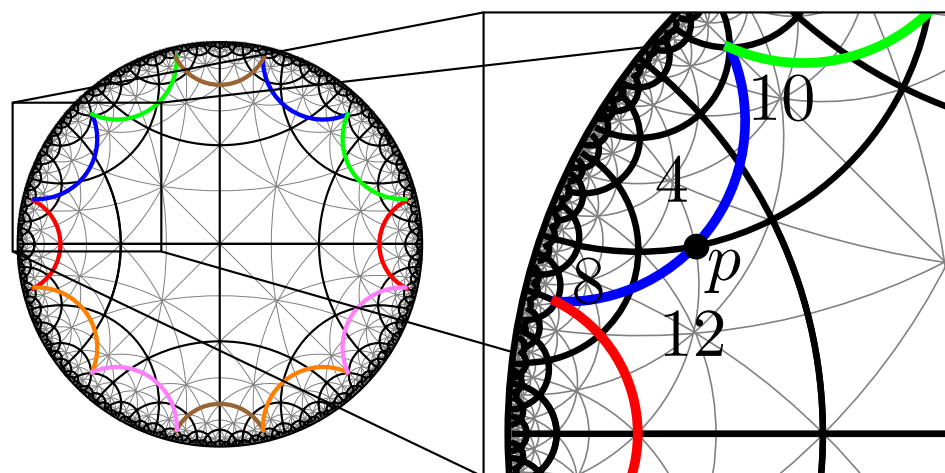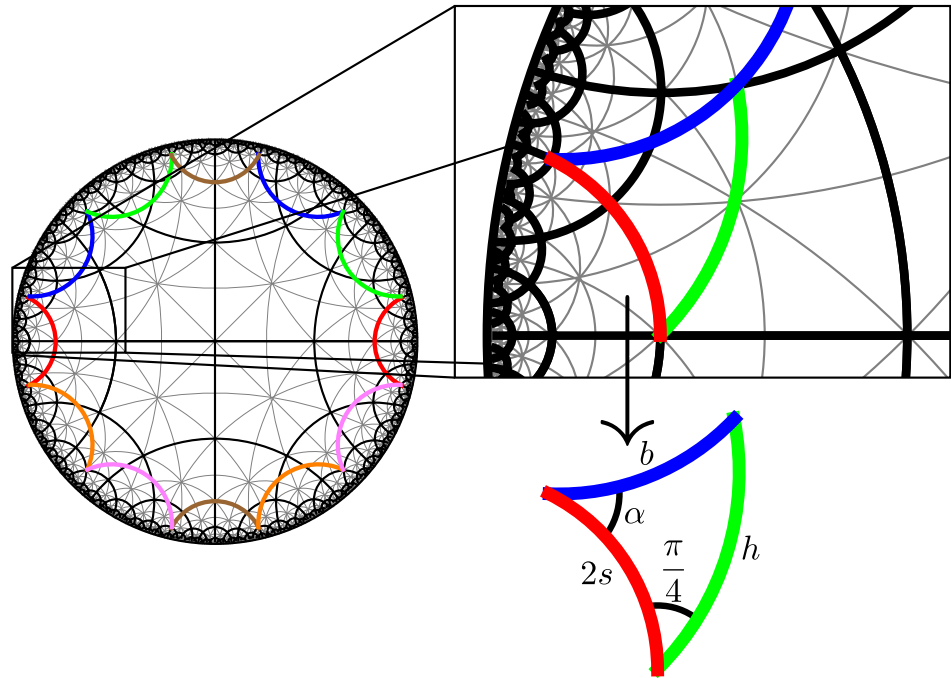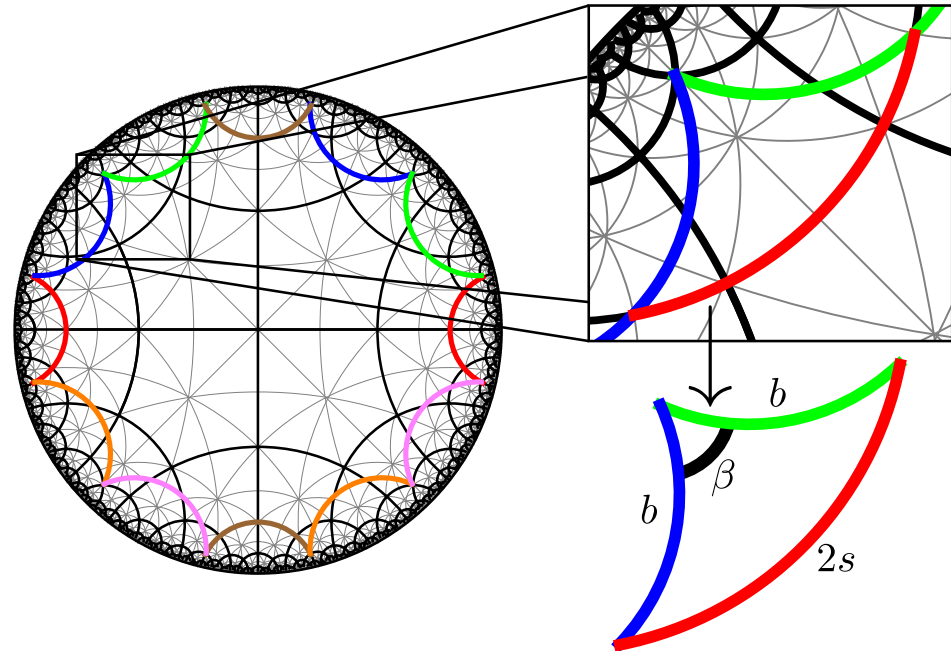

Figure 5.3.20: The point p is the midpoint for the blue edge.

Figure 5.3.21: How to find the length of b as well as α.

Figure 5.3.22: How to find β.

5.4   Information on Other Adinkra Embeddings

We have shown in section 5.1 that we understand the geometry of all adinkras of degree $N \geq 4$. So we can calculate the edge lengths of the embedding even if we do not know how the embedding looks like.

Proposition 5.4.1. *Let A be an adinkra of degree N, where $N > 4$. Let e be the length of an edge of A. Then the angle between pairs of edges is $2\pi/N$, and*

$$e = \cosh^{-1}\left(\cot^2 \frac{\pi}{N}\right).$$

Proof. Since the adinkra has N edges attached to each vertex and we know that angles between pairs of edges are equal, so the angle is indeed $2\pi/N$.

Since the degree of A is greater than 4, we have that the adinkra embeds into a hyperbolic surface.

At each square face, we can draw geodesic lines from the center of the square to the vertices. This turns each face into 4 triangles whose three interior angles are $\pi/N, \pi/N, \pi/2$. We can now use the dual hyperbolic law of cosines to get that

$$\cos \frac{\pi}{2} = -\cos \frac{\pi}{N} \cos \frac{\pi}{N} + \sin \frac{\pi}{N} \sin \frac{\pi}{N} \cosh e.$$

This implies that

$$\cosh e = \cot^2 \frac{\pi}{N},$$

and the result follows. □

Example 5.4.2. We have not figured out an embedding for the $N = 6$, but we can calculate the edge length of the adinkra after embedding to be $\cosh^{-1} 3$.   ◇

We will now talk about other ways of graph embeddings and how adinkras come in. Recall that a graph embedding into a surface is determined by cyclic orderings of the edges

attached to each vertex of a graph. We can easily conclude that there exist more than one way to embed the same graph onto some surface.

Definition 5.4.3. The *minimal genus* of a graph is the lowest integer n such that the the graph can be 2-cell embedded in a surface of genus n.   △

Definition 5.4.4. The *maximum genus* of a graph is the largest integer n such that the the graph can be 2-cell embedded in a surface of genus n.   △

Our adinkras are in fact embedded into the surfaces of minimal genus as shown in the following proposition.

Proposition 5.4.5. *The minimal genus that can come from an adinkra when embedded onto a surface is when all of the faces are quadrilaterals.*

Proof. From proposition 3.1.3, we have the relationship $2 - 2g = V - E + F$. This implies that

$$g = \frac{-V + E - F}{2} + 1.$$

Let A be an adinkra. This adinkra has 2^n vertices. Each vertex has N edges. So the total number of edges is $\frac{N2^n}{2} = N2^{n-1}$.

Now we will count the number of faces. Let x_k be the number of k-gons. Thus,

$$F = \sum_k x_k.$$

We will note that at each vertex, we must attach exactly N faces. Each k-gon will be attached to k vertices. Thus, we get the relation

$$N2^n = \sum_k kx_k.$$

Using algebraic manipulation, we get that

$$\frac{N2^n - \sum_{k>4}(2k - 4)x_k}{4} = \sum_k x_k.$$
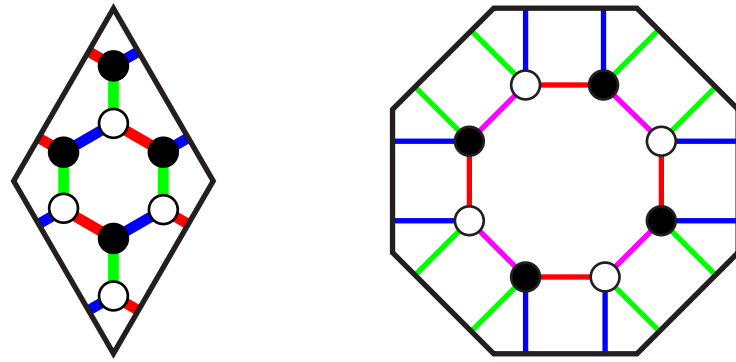
Figure 5.4.1: The left is an embedding of the cube adinkra into a torus. The right is an embedding of $K_{4,4}$ into a two holed torus, where the opposite edges of the octagon are identified.

Note that the right hand side is F. Thus, substituting in for the genus, we get

$$g = \frac{-2^n + N2^{n-1} - N2^{n-2} + \sum_{k>4}(k/2 - 1)x_k}{2} + 1.$$

Note that the value of g does not depend on the number of quadrilaterals. However, whenever we have at least one polygon with the number of sides greater than 4, the value of g increases. Thus, g is at its lowest value when there are only quadrilaterals. $\square$

While we do have a canonical way of embedding an adinkra into a surface, we can still try to find other ways of embedding the adinkra topology into a surface. For example, in figure 5.4.1, we have an embedding of a $n = 3, N = 3$ adinkra into a torus, when it normally embeds into a sphere, and we have another embedding of the $n = 3, N = 4$ adinkra into a 2-holed torus. We get these embeddings by attaching non-quadrilateral faces.

We proved that the adinkra edges are geodesics and all angles between pairs of edges are equal. With these embeddings, this can no longer necessarily apply. We find a counterexample to show that in fact, there are situations that lead to issues. We repeat once again, in figure 5.4.1, we have an embedding into a 2-holed torus, so the complex structure of the surface is hyperbolic. At each vertex, 2 octagons and 2 quadrilaterals are attached. If

we assume that all angles between pairs of edges are equal, we have that the quadrilateral has 4 right angles, which cannot exist in the hyperbolic plane. As a result, we do not understand the geometry of these embeddings at all. Looking into these embeddings is a possibility for continuation.

We end with two questions.

1. What is the maximal genus embedding of an adinkra?

2. How do we figure out the geometry of these non-minimal genus embeddings of adinkras?

Bibliography

[1] Mark J. Ablowitz and Athanassios S. Fokas, *Complex Variables: Introduction and Applications*, Cambridge University Press, Cambridge, 2003.

[2] William M. Boothby, *An Introduction to Differentiable Manifolds and Riemannian Geometry*, Academic Press, San Diego, California, 1987.

[3] James W. Cannon, William J. Floyd, Richard Kenyon, and Walter R. Parry, *Hyperbolic Geometry*, Flavors of Geometry **31** (1997), 59–115.

[4] Charles Doran, Kevin Iga, and Gregory Landweber, *An Application of Cubical Cohomology to Adinkras and Supersymmetry Representations* (2012).

[5] Charles Doran, Kevin Iga, Gregory Landweber, and Stefan Méndez-Diez, *Geometry of N-Extended 1-Dimensional Sypersymmetry Algebras* (2013).

[6] C. F. Doran, M. G. Faux, S. J. Gates Jr., T. Hübsch, K. M. Iga, G. D. Landweber, and R. L. Miller, *Codes and Supersymmetry in One Dimension* (2011).

[7] Ernesto Girondo and Gabino Gonzales-Diez, *Introduction to Riemann Surfaces and Dessins d'Enfants*, Cambridge University Press, Cambridge, 2012.

[8] Jonathan L. Gross and Thomas W. Tucker, *Topological Graph Theory*, Courier Dover Publications, 2001.

[9] Allen Hatcher, *Algebraic Topology*, Cambridge University Press, Cambridge, 2002.

[10] Frank Herrlich and Gabriela Schmithüsen, *Dessins d'enfants and Origami Curves*, Handbook of Teichmüller Theory **II** (2009), 767–809.

[11] W. Cary Huffman and Vera Pless, *Fundamentals of Error Correcting Codes*, Cambridge University Press, Cambridge, 2003.

[12] Gareth A. Jones, *Maps on surfaces and Galois groups*, Mathematica Slovaca **47** (1997), 1–33.

[13] Svetlana Katok, *Fuchsian Groups*, The University of Chicago Press, Chicago, 1992.

[14] William S. Massey, *Algebraic Topology: An Introduction*, Graduate Texts in Mathematics, 1967.

[15] Katsuhiro Matsuzaki and Masahiko Taniguchi, *Hyperbolic Manifolds and Kleinian Groups*, Oxford University Press, 1998.

[16] Rick Miranda, *Algebraic Curves and Riemann Surfaces*, American Mathematical Society, Providence, Rhode Island, 1995.

[17] Bojan Mohar and Carsten Thomassen, *Graphs on Surfaces*, John Hopkins University Press, Baltimore, Maryland, 2001.

[18] James R. Munkres, *Topology*, Pearson Education, Upper Saddle River, New Jersey, 2000.

[19] Jacqueline A. Stone, *Generalized Adinkra Homology*, 2011, `http://digitalcommons.bard.edu/senproj_s2011/3`.

[20] William P. Thurston, *Three-Dimensional Geometry and Topology*, Princeton University Press, Princeton, New Jersey, 1997.

[21] Yan X. Zhang, *Adinkras for Mathematicians*, Transactions of the American Mathematics Society **366** (2014), 3325–3355.